Multi-objective optimisation framework for designing office windows: quality of view, daylight and energy efficiency

Peiman Pilechiha[1], Mohammadjavad Mahdavinejad[1], Farzad Pour Rahimian[2,3,*], Phillippa Carnemolla[4], Saleh Seyedzadeh[5]

[1] Department of Architecture, Tarbiat Modares University, Tehran, Iran

[2] School of Computing, Engineering & Digital Technologies, Teesside University, Tees Valley, Middlesbrough, UK

[3] Department of Civil and Environmental Engineering (DICeA), University of Florence, Florence, Italy

[4] Faculty of Design, Architecture and Building, University of Technology Sydney, Australia

[5] Faculty of Engineering, University of Strathclyde, Glasgow, UK

[*] f.rahimian@tees.ac.uk

CE2.20, Orion Building, Stephenson St, Tees Valley, Middlesbrough TS1 3BA, UK

Abstract

This paper presents a new, multi-objective method of analysing and optimising the energy processes associated with window system design in office buildings. The simultaneous consideration of multiple and conflicting design objectives can make the architectural design process more complicated. This study is based on the fundamental recognition that optimising parameters on the building energy loads via window system design can reduce the quality of the view to outside and the received daylight – both qualities highly valued by building occupants. This paper proposes an approach for quantifying Quality of View in office buildings in balance with energy performance and daylighting, thus enabling an optimisation framework for office window design. The study builds on previous research by developing a multi-objective method of assessment of a reference room which is parametrically modelled using actual climate data. A method of Pareto Frontier and a weighting sum is applied for multi-objective optimisation to determine best outcomes that balance design requirements. The Results reveal the maximum possible window to wall ratio for the reference room. The optimisation model indicates that the room geometry should be altered to achieve the lighting and view requirements set out in building performance standards. The research results emphasise

the need for window system configuration to be considered in the early design stages. This exploratory approach to a methodology and framework considers both building parameters and the local climate condition. It has the potential to be adopted and further refined by other researchers and designers to support complex, multi-factorial design decision-making.

Keywords:

Multi-objective Optimisation; Quality of views; Window design; Daylight; Building energy usage, Office Design

Highlights:

- Multi-objective optimisation of energy performance associated with window design
- Simultaneous and conflicting objectives are considered helping simpler comparisons
- A framework for numerical assessment of view in office environments is proposed
- View, energy performance and daylighting are considered as optimisation objectives
- The best model found has highest view and daylight, and medium energy consumption.

1. Introduction

Artificial lighting contributes to a large proportion of electricity consumption in commercial buildings across the globe. For example, in the US, artificial light lighting contributes to one-third of electricity consumption in commercial buildings [1]. In the UK, this sector accounts for almost 24 million tons of carbon dioxide per year (equal to 47% of the CO2 emission of the UK) [2]. In Iran, artificial lighting is responsible for 25% of electricity usage in office buildings [3]. This level remains relatively high despite Iran having a high daylight availability during working hours (Tehran has an average of 8.5 sunshine hours per day). In light of a global recognition of the importance of more sustainable and efficient building performance, it is therefore important to develop methods to minimise the electricity usage for lighting through best practice design decisions. One efficient method is to utilise the natural daylight in indoor areas more effectively. To achieve this, a considered design approach to the placement and size of windows in office buildings is imperative.

Several studies have examined the effect of daylight on occupant behaviour [4], increasing productivity [5] and also job satisfaction of employees [6] and their health conditions [7]. Studying the lighting conditions in office types shows strong relationships between the illuminance at eye level and the health parameters, namely fatigue and sleep quality [8]. It was concluded that even the colour temperature of light has significant correlation with the performance and alertness of office workers [9]. It has been shown that not only daylight has direct physical effects on occupants, but also physiologically it is an efficient energiser to human visual and circadian systems [10]. However, daylight can also cause visual discomfort through glare and distraction [5]. Hence, the productiveness of the daylight for visual efficiency depends on how it is delivered, and it is recommended that direct sunlight should be avoided in areas in which visual activities are required [11]. The views and perspectives provided by windows have been shown to impact both the visual performance and the comfort of workers [12]. The positive effects of a pleasant or attractive view in the workplace include reduced physical and psychological discomfort, enhanced sleep quality [13] and eye health [14] and increase job satisfaction [15].

As such, the optimisation of window design, especially in commercial buildings, involves the careful balancing of three main objectives: maximising energy efficiency through natural lighting, while providing the best possible view and optimum visual comfort. Many efforts have considered window type, size, and glazing in their calculations to optimise various objectives as life cycle cost and life cycle environmental impact [16], energy efficiency and occupant's comfort [17], and retrofit actions [18] However, this approach provides architects with restricted information, and many other design objectives might be compromised. To address this issue, several researchers focused only on daylighting and thermal efficiency [24] considering window glazing [19], external shading [20] and window size, orientation, and wall reflectance [21], some others investigated visual comfort and energy performance together focusing on the orientation of windows [22], window size [23], exterior components [24] and whole building characteristics [25]. Iommi [26] evaluated daylighting performance and visual comfort in specific buildings. However, these interdependent factors have not been simultaneously considered in the building design. One reason for this is the subjectivity of assessing visual comfort, which is a case-based quality based on a person’s individual experience of architecture [27]. Another barrier has been the need to consider of all objectives and the resultant increase in complexity of the design decision-making.

To address the challenge mentioned above, this study proposes a framework for evaluation of Quality of View (QV) in office buildings and applies a multi-objective optimisation method to minimise the energy consumption and maximise the daylight and visual comfort (absence of glare). The objectives of minimisation of energy consumption and Annual Sun Exposure (ASE) and also maximisation of daylight are assessed using simulation software, whilst the target values of the objective of QV are input using the proposed framework. This research applies the framework to a case study of a typical office building located in Tehran city, Iran, to determine the most appropriate window dimensions and positions.

The paper is structured as follows; first, a review of previous studies and issues with building windows design in the optimisation of energy efficiency, daylighting and visual comfort is presented. This is followed by explanation of the proposed methodology along

with the developed framework for the analysis of view quality. The results from the application of the suggested multi-objective optimisation method in the studied case are then reported, followed by a discussion of the criteria for selection of the best solution from the generated Pareto front. The final section summarises the article and contains highlights of the main knowledge contributions and recommendations on the future works.

2. Background and Motivation

This study aims to develop a protocol for the optimisation of office window design (position and area), which targets the minimisation of energy usage and the optimisation of daylight and visual performance. Criteria to asses these objectives are broadly discussed in the seminal literature. Therefore, the first part of the literature review in this paper is dedicated to the review of studies that have developed evaluation indices for the optimisation process to enhance integrated building design. The second part discusses the body of evidence that addresses the optimisation of window design and challenges within the field.

2.1. Performance goals and building design indices

Building openings, windows [19], and doors or generally all key elements of building façades [28], allow for daylighting, visual connection to the outside and also heat penetration. Windows directly contribute to building energy usage in two ways. Firstly, heating, from direct sunlight through windows, imposes high cooling loads in warm seasons. Secondly, in cold seasons, the heat loss from windows is significant, because of the high thermal transmittance of glazing (represented as a higher U-value) when compared to (non-glazed) walls. Hence, a critical factor in the design of energy-efficient buildings is the design of a window system that takes into consideration the impact of high thermal transmittance of glazing [29]. User comfort is another factor to be considered in estimating energy performance, using various indexes and prognostic methods [30, 31]. Ochoa *et al.* investigated the suitability of combined optimisation criteria on window sizing methods for low energy consumption focusing on user visual comfort and performance [23]. Ghaffarianhoseini *et al.* investigated the ability of vegetation [32] or unshaded courtyards [33] for contributing to outdoor thermal comfort based on various design

configurations and scenarios. Rupp *et al.* [citation ?] revealed that there is a gap in thermal comfort studies in relation to interdisciplinary research, and a connection with other related fields such as psychology, physiology, and sociologists could be of great asset for the development of an integrated research approach aiding a better understanding about perception and thermal comfort and its physiological and psychological dimensions [34]. Khatami and Hashemi investigated the influences of decreasing internal heat gain and introducing automated ventilation strategies into lightweight open-plan offices to improve energy performance thermal comfort and indoor air quality [35].

There are a number of methodological approaches to predict and model the thermal behaviour of buildings. One way is by using a simplified physical model [36] based on thermodynamic laws, heat transfer and thermodynamic variables. The 'degree days' approach is another method which uses a measure of local outside temperature over time to calculate energy consumption required to heat or cool buildings [37].

A number of sustainable certification systems [including Building Research Establishment Environmental Assessment Method (BREEAM) [38] and Leadership in Energy and Environmental Design (LEED)] have been developed to continually assess energy performance across all life stages of a building, and have been designed to incentivise better design and analysis of low energy-consuming building systems, whether by classical [39] or even machine learning [40] methods. The analysis of indoor daylight performance is generally performed using software simulation calculating a range of metrics e.g. Daylight Illuminance (DI), Daylight Factor (DF), Daylight Coefficient (DC), Daylight Autonomy (DA) [41] and ASE [42]. The metrics of Spatial Daylight Autonomy (sDA) and ASE are the most common daylight indices used in the LEED 4 rating.

Daylight Illuminance (DI) is the most common daylight performance measure, which designates the brightness of the daylight in illuminating the indoor environment. The unit for DI is lux. Based on the application of each environment, the recommended illuminance level might be different. For instance, an illumination level higher than 500 lux is suggested for an office [43] and a range between 200 to 500 lux for a classroom [44].

DF is determined as the ratio of the daylight illuminance at an indoor point to the illuminance at the same outdoor point under the sky. DF is a traditional approach to

evaluate the daylight illuminance inside a building and mostly used due to simplicity [48]. Nonetheless, using DF metrics may lead to an inaccurate calculation because the ratio of internal to external illuminance diversifies considerably in a real situation. Moreover, the impact of direct sunlight is ignored in this method [45]. DC approach was developed to propose a more practical measure in comparison with the DF. It considers dynamic changes in the luminance of the sky elements under various sky conditions and solar positions [46]. The assumption is that the sky is divided into several patches, contributing to the internal illuminance level at a point [47]. Hence, the calculations are time-consuming and complicated [48].

DA which is also referred to as dynamic daylight metric is a climate-based metrics, determined as the percentage of annual daytime hours of the year, when a specific illuminance threshold is achieved, by daylight alone [49]. The assessment of sixty architecture students works revealed that DA is the most accurate daylight measurement. The continuous DA (cDA) and DA_{max} are two modified versions of DA. The former metric assigns the partial participation of daylight to illuminance when it is lower than the minimum threshold. Whereas, the second one indicates the percentage of the time when daylight illuminance is ten times the recommended illuminance; beyond which condition the risk of glare from direct sunlight patch would rise [50].

sDA describes the annual amount of self-sufficiency in the environment, in terms of the amount of daylight received in the interior, and is the ratio of the analysed space, with the minimum received brightness defined for the desired activity during working hours of a year. According to the simulator's opinion, analysis can only include the working area, but usually, the total space is considered. Assume a grid of *N* points, and assign a function ST*(i) whose value becomes one* for every point *i* in the grid getting the minimum required illuminance for more than the given fraction of total occupancy time, the sDA can be represented as:

$$sDA = \frac{\sum_{i=1}^{N} ST(i)}{N} \; with \; ST(i) = \begin{cases} 1: st_i \geq \tau t_y \\ 0: st_i \leq \tau t_y \end{cases} \quad (1)$$

Where st_i denotes the occurrence count of exceeding the sDA illuminance threshold at point *i,* t_y is the annual timestamp count and τ represents the temporal fraction threshold.

Illuminating Engineering Society (IES), which introduced the idea of the sDA [42], set the minimum illumination of 300 lux for 50% of the year when the zone was occupied (from 8 am to 6 pm), which is written as $sDA_{300/50\%}$. IES also has provided two categories for sDA [42]. In order to have preferred daylight sufficiency in space, at least 75% of the analysed points should receive more than 300 lux in at least 50% of the year when it is occupied (3 points). Nominally accepted, the brightness of more than 300 lux in 50% of the time of the year is considered for at least 55% of points (2 points) [42]. These recommendations are based on the comparison of occupants' opinions with the results of daylight simulations [51]. The most important advantage of the DA family compared to the other daylighting indices is that the annual daylight performance assessing is done, with regards to the sun and sky condition based on meteorological climatic data. These indices help designers understand the overall conditions of daylight in buildings over a period of one year. Given the fact that these data are recorded continuously (prediction is based on continuous daytime measurements), it is often difficult to assess the instantaneous light situation with the DAs. Also, DAs are based on the percentage of occupied space per year and do not take into account the changes in hourly light, which is one of the most important aspects of building design. Where the sDA index is estimated to be the same for different models, a more accurate analysis can be made using the DA_{ave}.

ASE is the ratio of analysed space that receives more than a certain amount of direct sunlight in a number of specific hours of the year. Both factors determination (number of hours and amount of radiation) in the index definition is required. IES Recommendation is $ASE_{1000,\ 250h}$, which is the percentage of space in which in more than 250 hours of the year, the direct exposure of the sun is more than 1,000 lux. Similar to sDA, ASE can be mathematically represented as:

$$ASE = \frac{\sum_{i=1}^{N} AT(i)}{N} \; with \; AT(i) = \begin{cases} 1: at_i \geq T_i \\ 0: at_i \leq T_i \end{cases} \quad (2)$$

Where at_i is the occurrence count of exceeding the ASE illuminance threshold at the point *i* and T_i represents the annual absolute hour threshold.

The LEED ver.4 requires the attention of designers to the ASE and sDA to score 2 to 3, respectively by reaching 55-75% of the area of the occupied spaces. To achieve this goal, designers using annual computer simulations need to show that the annual direct solar radiation of $ASE_{1000,\ 250h}$ is received in less than 10% of the space. It is necessary that simulation run based on $sDA_{300/50\%}$.

Among all the window-related properties, the most appealing and challenging one is the view to outdoor. In the property market, there is a direct relationship between the value of the high-rise building [52] or a neighbourhood [53] and the pleasant outdoor view. There is also evidence that views can positively impact on eye health [54], wellbeing [55] and comfort [56]. Being able to see natural landscapes from inside a workplace building has a significant impact on reducing stress and increasing individual attention. Researchers' studies demonstrate that the relationship between view and daylight in contemporary facades is less perceptible, and the indices and studies related to view are very limited [57]. Interestingly, only the LEED v4, the Chartered Institution of Building Services Engineers (CIBSE), as well as the New European Daylighting Standard EN 17037, have introduced design guidelines for achieving a desired view to outdoor.

The basis of LEED v4 [58] for meeting QV needs, is to provide a direct view through the view glazing for 75% of the occupied space and seeks to enhance the connection between the perimeter environment and the building occupants. In addition to having 75% of the occupied space in the index, these parts must also provide at least two of the following four view types. View type 1 is the horizontal and vertical viewing angles of at least 90 degrees to the view glazing. View type 2 is the viewing content of the two of the following three objects: the visibility of flora, fauna, or sky or movement. View type 3 is the distance from the window, which is less than three times the height of the window from the floor. View type 4 is a view factor (VF) of 3 or more. VF is categorised from zero to five based on the minimum horizontal and vertical angle of each point of occupied space than the window (user is sitting on chair and height of the eye is 1.2 meters). If this view angle is more than 50 degrees, the rate of 5 is granted (table 4). VF of 3 and higher means a view angle of at least 11 degrees [42].

The UK-based CIBSE provides methods for assessing view based on the position of the observer in space [59]. This standard evaluates the quality of view based on four factors: window width, the distance of the view, view layers (sky, landscape, and foreground) and environmental information (contents). The view quality is rated based on four levels: unacceptable/acceptable/good/excellent. The New European Daylighting standard EN 17037 has recently introduced three general principles of horizontal viewing angles, distances and visibility levels, which is similar to the standard of the CIBSE. According to its categorisation, the horizontal angle of at least 14 degrees as a minimum, more than 28 degrees is average, and the angle more than 54 degrees is maximum. Also, the window distance from the obstacle of more than 6 meters is minimum, more than 20 meters is medium and more than 50 meters is maximum. Visible layers could be the sky, landscape, or earth, and if at least one of them is visible, the minimum score is achieved. The average score is for the view to two layers, and if all layers can be covered, a maximum score will be obtained [60].

Therefore, view angles, view contents, a distance of the view and observer position are some indices considered in recent regulations. Among these indices, simulating some of them are very difficult or impossible due to differences in the models, such as view content simulation or view layouts and also environmental information. As such, this paper focused on other measurable indices.

To date, there is no tool that simulates view based on these indicators. For example, recent versions of DIAL+ software, built to assess the new daylight requirements of EN-17037 [51], do not optimise the objectives of standard and perform view simulations that assess only one of the three conditions of the standard. Therefore, there is an opportunity to develop a tool to simulate the view based on the LEED v4 guidelines.

2.2. Related Studies

There is an established body of evidence which has built around optimising the design of window systems for a range of outcomes and objectives, some isolated single objectives, others combined objective optimisation. Lee *et al.* [61] investigated different types and characteristics for the window systems, to optimise energy usage. This study was limited to assessing energy performance in isolation, however, did consider a specific

climate in the proposed approach. Futrell *et al.* [62] examined a process of optimising the thermal and lighting performance of a typical classroom and investigated the orientation of windows. The results revealed that thermal and lighting performance was strongly conflicting in a north orientation, (research based in the United States – northern hemisphere). Mangkuto *et al.* [21] also investigated different characteristics of window systems including a Window to Wall ratio (WWR), wall reflectance, and window orientation on daylight metrics and lighting electricity consumption. Mangkuto's research studied an office room in a tropical climate and was one of the first to demonstrate the possibility of incorporating the view/visual aspects of window systems into an optimisation process.

Ochoa *et al.* [23] also employed an optimisation approach to identify the window size while optimising energy consumption and visual comfort. Vanhoutteghem *et al.* [63] discovered the suitable window solution for various room sizes by assessing the impact of the window design variables on the thermal performance and comfort as well as daylighting using a contour plot.

Liu *et al.* [64] studied the feasibility of an optimisation workflow for the cooling and heating load of a residential building with changing in spatial form and building envelope parameters. They verified the optimisation results achieved by Octopus comparing with the average objective values and also did correlation analysis between design parameters and performance.

Fang *et al.* [65] optimised simple building geometry, window and skylight size and placement for energy and daylighting performance. The genetic algorithm utilised to increase more than 28% in daylight performance and decrease more than 17% in energy consumption in different climates. Dino *et al.* [66] developed a design optimisation tool to support high-performance building design and employed it to buildings' energy and daylighting performance optimisation in different layout designs and building openings.

Zhai *et al.* [67] applied a multi-objective optimisation algorithm to minimise the energy use and to improve the visual and thermal comfort of a reference office room by finding the most appropriate parameters for the window system. These factors include WWR, outer and inner glass metrical and the filling gas. Although the recommendations show

remarkable improvements in the target values, the results are very restricted, as it ignored the climate and orientation.

Hiyama *et al.* [68] proposed a method to reduce the number of required simulation for optimisation of the window geometries and electric energy usage, by creating response surfaces, between those targets and likening DF and cDA.

As well as being incorporated into optimisation processes, the outside view has been considered in the proposed decision-making tool, for early design phases in adaptive façade [69] or developing an automated shading control [70]. However, most of these works only considered quantitative measures for this objective (i.e. achieving maximised WWR). As indicated by seminal works, an assessment tool for simulating view performance is a valuable addition to properly design a window system – and one that is currently lacking in the evidence. The lack of integration of outside view as a measure in optimisation of window system designs is a gap that has been identified in the literature, especially in office environments.

2.3 Research Gap

Designing modern buildings requires consideration of many different trade-off factors. Whilst there is an expectation that buildings should provide comfort and support the well-being of their users, buildings must also perform sustainably throughout their life-cycle, and the minimisation of energy use is one of a range of factors that are increasingly valued and expected, a value reflected in building regulations and requirements.

Architects and decision-makers need decision-making tools to be enabled to effectively balancing competing factors. Window design is a particularly complex optimisation task due to its contribution to building energy performance, daylighting and QV, particularly in office spaces. As the survey of literature in this section shows, there are ample researches optimising a combination of the two objectives, which are mostly daylighting and energy usage. QV is notably absent as a window design objective being measured or considered.

Based on the literature, a comprehensive optimisation approach faces two main challenges: lack of a method to properly evaluate QV as numerical values and the interoperability of assessing tools. This paper, therefore, lays out a widely-applicable

framework to assess the QV in the office environment and an approach to consider three main factors in designing windows.

3. Research Methodology

This study applies a multi-objective optimisation method with the aim of maximising the energy performance, daylighting and the quality of view to outside of an office environment, across different window system scenarios. The following paragraphs outline the research methodology, optimisation algorithm, as well as the studied and utilised tools.

3.1 Multi-objective optimisation

Multi-objective optimisation differs from a single objective enhancement primarily in its increased complexity, a direct result of the complicated nature of simultaneously satisfying several goals, often with competing outcomes. In order to accurately optimise multiple objectives, a set of circumstances that define the optimal solutions must be defined, and a Pareto frontier generated. Within these set of circumstances, all points within this set (also called non-dominated or feasible solutions), are logically valid and result in various values of the objectives. Generally, in most applications, including building design, only one best solution is required by decision-makers.

The criteria to select the final point, from the non-dominated points, differs for each application. The representations for describing different objectives under the investigation can be related to the maximum or minimum functions. However, the two extreme points can be transferred to each other, by the following formula:

$$\max\{f(x)\} \Leftrightarrow \min\{-f(x)\} \tag{3}$$

Then, mathematically a multi-objective optimisation problem can be expressed as:

Minimise:

$$F(\vec{x}) = [f_1(\vec{x}), f_2(\vec{x}), \dots, f_m(\vec{x})]^T \tag{4}$$

Subject to

$$g(\vec{x}) \leq 0$$

$$h(\vec{x}) = 0$$

where

$$x_i^{min} \leq x_i \leq x_i^{max}\ (i = 1,2,\dots,n)$$

$$x = [x_1, x_2, \dots, x_n]^T \in \Theta$$

$$y = [y_1, y_2, \dots, y_m]^T \in \psi$$

Here *m* is the number of objective functions, which is three in the case of the problem investigated in this study. Φ is the search space with *n* dimensions and identified by upper and low bounds of the decision variable $x_i(i = 1,2,..,n)$.

$$x^{max} = [x_1^{max}, x_2^{max}, \dots, x_n^{max}]^T \quad (5)$$

$$x^{min} = \left[x_1^{min}, x_2^{min}, \dots, x_n^{min}\right]^T \quad (6)$$

Ψ is the *m*-dimensional vector space of objective functions and is defined by Θ and the objective function *f(x)*. $g_j(\vec{x}) \leq 0(j = 1,2,..,p)$ and $h(\vec{x}) = 0(j = 1,2,..,q)$ denotes *p* and *q* which are respectively the number of inequality and equality constraints. If both *p* and *q* are equal to zero then the problem is simplified as an unconstrained optimisation problem.

Figure 1 presents an example of a Pareto frontier for the optimisation of two simultaneously conflicting objectives. The Pareto solutions have been surrounded by a vector of an ideal solution and a vector of dominated solutions, determining the upper and the lower bounds of optimal solutions. An ideal or utopia point is a hypothetical concept with reference to a perfect target in which each objective is optimised without paying attention to the satisfaction of the others.

Multi-objective optimisation algorithms attempt to generate solutions that are as close to the Pareto optimal front with a possible uniform distribution. When the non-dominated solutions are identified, decision-makers choose from this set a final resolution according to the particular problem and personal preferences.

A hypervolume-based evolutionary optimisation (HypE) algorithm is utilised in this study, due to its effectiveness compared to other multi-objective optimisation techniques [71]. HypE is an evolutionary multi-objective algorithm which features hypervolume indicator [72], non-dominated sorting, and a fast search method based on Monte Carlo simulation [73].

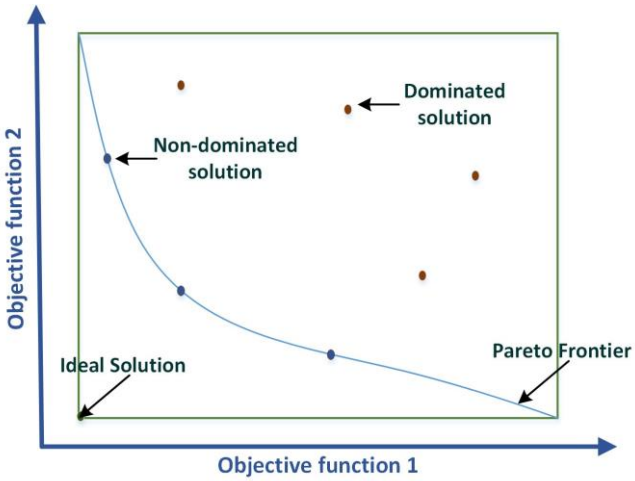

Figure 1- An example Pareto frontier of a multi-objective optimisation.

The optimisation method is applied using Octopus [74], a plug-in of Grasshopper [75], which is used for creating models for energy performance simulation analysis. The hypervolume indicator of a point set is determined as the volume of the region dominated by the point set and bounded by a reference point. Hence, it is crucial to carefully define this reference point. If this point is too close to the Pareto front, it will cause incomplete cover of the non-dominated set, and if it is too far from the Pareto front, it will lead to low accuracy in Monte Carlo simulation. The HypE algorithm developed in Octopus uses a dynamic reference point based on normalisation and slight changes in objective values.

3.2. Application to a case study

3.2.1 The studied case for the simulation model

A reference office room for the case study is adapted from a standardised specification defined in a previous research paper [76] which consists of single-zone working space, with dimensions of 3.9 m × 8.5 m × 2.8 m (Figure2). The room is located in the middle

floor of a multi-story building, with an approximate area of 2300 m^2. It is enclosed by other office rooms, except for the façade which is faced to the south (Figure 2). Hence, the façade is considered diabatic and the rest of the wall as adiabatic. The input parameters for this case study are summarised in Table 1.

Table 1- Input parameters of the research base model

parameter	value
interior wall thickness	0.15 m
floor to floor distance	3.10 m
occupied period	8 am to 6 pm
heating and cooling setpoints	20 and 26 °C
heating and cooling Setback	15 and 30 °C
peak occupant load	7.38 m^2/ppl
lighting power density per area	10.1 W/m2
peak plug loads*	8 W/m^2
infiltration rate per area**	0.0006 $m^3/s\text{-}m^2$
ventilation per area	0.00045 $m^3/s\text{-}m^2$

*: one Energy Star-rated LCD monitor and laptop per occupant present

**: according to ASHRAE recommendation for Leaky building and poor construction details in the research context

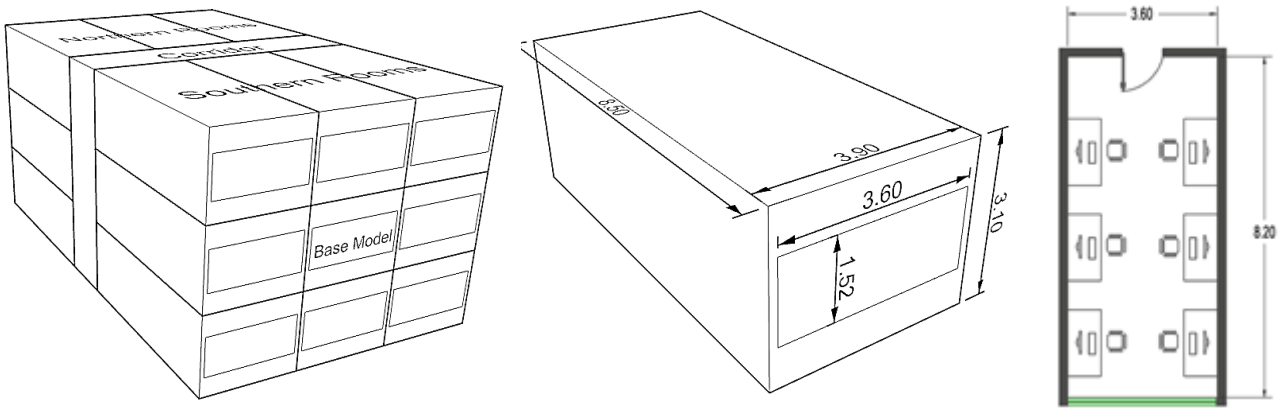

Figure 2- research model and other multiple reference offices stacked to it.

The Heating, Ventilation, and Air Conditioning (HVAC) system for such a building is considered packaged rooftop VAV (Variable air volume), with reheat based on ASHRAE 90.1 [77] recommendations. In this system, fan control is Variable Air Volume (VAV), the cooling type is chilled water and heating type is hot-water fossil fuel (natural gas) boiler.

The annual mean Coefficient Of Performance (COP) for this system is considered 3.02 for the cooling system and 0.8 for natural gas boiler and 1.0 for conventional electric resistance for >70kW and <223kW cooling capacity based on ASHRAE/USGBC/ANSI 189.1 [78].

The walls are finished in white plaster, the floor is covered with grey tiles, and ceilings are white. Exterior Walls layers are, out to in, Mortar 0.03 m, Hollow brick 0.15 m, EPS (Expanded Polystyrene) 0.10 m, Plaster 0.03 m. Other materials characteristics are shown in Table 2. These materials are considered common construction materials in buildings in Tehran's official buildings. The total U-value is for the exterior wall is 0.329 W/m^2K and the reflectance is 50% inside and 35% outside. The interior wall reflectance is considered 50%. The reflectance of the ceiling and floor is 80% and 20% respectively. All surfaces except one on façade, are considered adiabatic.

Glazing consists of double clear glass with air in the middle based on ASHRAE 169 [79] for cities in climate zone 3B. The SHGC, U-Value, and VT for such glazing are 0.25, 0.65 W/m^2K and 0.45, respectively.

Table 2-Characteristics of construction materials in research.

Material Name	Roughness	Conductivity	Density	Specific heat	Thermal emittance	Solar absorptance	Visible absorptance
		W/m.k	kg/m^3	J/kg-K			
Mortar	Medium rough	1.0	1800	1840	0.9	0.6	0.6
Hollow brick	Medium rough	0.5	1300	840	0.9	0.7	0.7
Plaster	Smooth	0.4	900	1100	0.7	0.6	0.6
EPS	Medium rough	-	15	1340	0.9	0.6	0.6

3.2.1 Description of the climate regions

Geographically, the B category (dry) in the Köppen climate classification, accounts for 82.28% of Iran. In this research, Tehran is selected as an example of this climatic range. It has a dry climate with a little precipitation throughout most of the year. Actually, this is a hot semi-arid climate and receives a little more precipitation than the arid (desert) climate. This climate receives this precipitation from the ITCZ (inter-tropical convergence zone) or from mid-latitude cyclones. The weather files used in this research is for Mehrabad International AirPort with Latitude of 35.683 and Longitude of 51.317, located

in elevation of 1190.0 meters. The file is available to download from the EnergyPlus website [80]. The climate parameters are summarised in Table 3.

Table 3- Tehran climate parameters influencing research objectives. Data were sourced from the weather file provided by the EnergyPlus database for Tehran.

Whether data	unit	Hourly			average monthly	
		Average	Max	Min	Max	Min
Dry-bulb temperature	C	17.27	40	-5	30.07	3.88
Relative humidity	%	40.57	99	3	62.99	21.92
Dew point temperature	C	1.61	18.5	20.0	6.78	-3.5
Wind speed	m/s	2.71	16.3	0	4.25	1.67
Direct normal radiation	Wh/m^2	206.98	775	0	299.97	120.21
Diffuse horizontal radiation	Wh/m^2	121.15	540	0	177.11	64.73
Global horizontal radiation	Wh/m^2	244.25	1069	0	364.24	117.26
Horizontal infrared radiation	Wh/m^2	340.58	489.0	229.0	409.04	274.93
Total sky cover	tenth	4.44	9.0	0.0	4.60	4.24
Barometric pressure	Pa	87943.21	98300.0	86900.0	88416.26	87419.58

3.3 Optimisation objectives and simulation tools

The objective functions for the window system design problem are building energy loads for lighting, daylighting and view to the outside. For the simulation of the office room, the 3D graphics software Rhinoceros [81] and Grasshopper plug-in are employed to control the parameters. Parametric models are useful for design exploration in complex and dynamic design settings [82] which are window location and dimension in this study.

To quantify and evaluate annual daylighting performance, sDA and ASE metrics are utilised. These indices are contradictory to each other and it is not possible to calculate one metric for representing daylight. The Energy Use Intensity (EUI) metric is also used for assessment of the electricity usage, which represents the office energy consumption as a function of its conditioned floor area. So, EUI in this study is the sum of normalised heating, cooling, electric equipment and electric lighting load in a year ($Kwh/m^2/y$).

The view to the outside is assessed using the proposed QV metric (refer to Section 3.4). Hence, our optimisation process will consider four different functions are considered in our optimisation process.

The daylight and energy metrics, which were elaborated in Section 2.1 are calculated using Grasshopper plug-ins, namely Ladybug and Honeybee [83]. These simulation tools use EnergyPlus [84] and Open Studio [85] engines for energy simulations. To simulate the integrated daylight and energy simulation, lighting schedule has now been updated according to annual daylight luminance. Afterwards, this schedule (red arrow in figure 6) is imported into the energy model to incorporate the electrical lighting energy requirement differences due to daylighting. For the calculation of ASE, an extra algorithm is developed in Grasshopper, to use EnergyPlus weather file of Tehran and determine the direct illuminance in the horizontal plane, which is recorded at the end of each hour. Then the average illuminance for each hour is calculated. In the next phase, sun vectors are plotted for the hours, which is more than 1000 lux. Using these sun vectors, the hours in which the sunlight hits the test surface (similar to the one used in daylighting analysis) are simulated. With the number of hours of direct sunlight received by each of the test points in the test surface, the portion of the space below 250 annual hours is calculated.

As mentioned in Section 2, the view performance has been under-investigated in previous studies, therefore, this study is the first to develop a framework for quantification of this objective. The framework is elaborated in the next subsection.

The following optimisation objective function extended fitness functions that were introduced [86] and applied [87] earlier, in using the weighting method to accurately find the optimum solution in Pareto front solutions.

$$FF_i = (sDA_i - sDA_{min})C_1 - (ASE_i - ASE_{min})C_2 - (EUI_i - EUI_{min})C_3 + (QV_i - QV_{min})C_4 \quad (7)$$

Where:

i= result of iteration

Min= minimum value of optimisation set

Max= maximum value of optimisation set

$$C_1 = \frac{100}{sDA_{max} - sDA_{min}} \quad (8)$$

$$C_2 = \frac{100}{ASE_{max} - ASE_{min}} \quad (9)$$

$$C_3 = \frac{100}{EUI_{max} - EUI_{min}} \quad (10)$$

$$C_4 = \frac{100}{QV_{max} - QV_{min}} \quad (11)$$

Here, min and max values presents each objective's minimum and maximum values appeared in the solutions generated by the optimisation algorithm.

The fitness function was calculated for all Pareto front solutions, which results in diversity in EUI, daylight and view values. It should be noted that the equation (7) is different from the weighting method that converts multi-objective optimisation to single objective one. The difference is that in the latter the algorithm only optimises one function, but here, first four different objectives are optimised and then the fitness function is calculated over Pareto front to rank the solutions and conclude the best one [88].

3.4 Metrics for the view to the outside

To simulate QV in this research, a Python [89] based plugin for Grasshopper is used. The developed plugin is able to evaluate and visualise five view types based on observer positions throughout the space. To define the viewer positions, a user-defined grid on a view analysis surface is constructed. The view analysis surface is located at eye-height of a seated user and is shown with the blue dash line in perspective and also in room section in Figure 4.

The evaluated view types are view access, view angles, VF and view depth. With the results of these evaluations for the viewpoints, view quality could be assessed in two steps as per the LEED approach.

For N points on the view analysis surface, in the first step, view access is determined. In the second step, other view types are evaluated for each point passing the last step threshold. Finally, the viewpoints, which passed the first step and also 2 out of 3 other view type thresholds, are considered as points with the QV. Figure 3 shows the QV

assessment process for each point (i) on the view analysis surface. Therefore the QV value in this research is the percentage of viewpoints which pass these two steps (j).

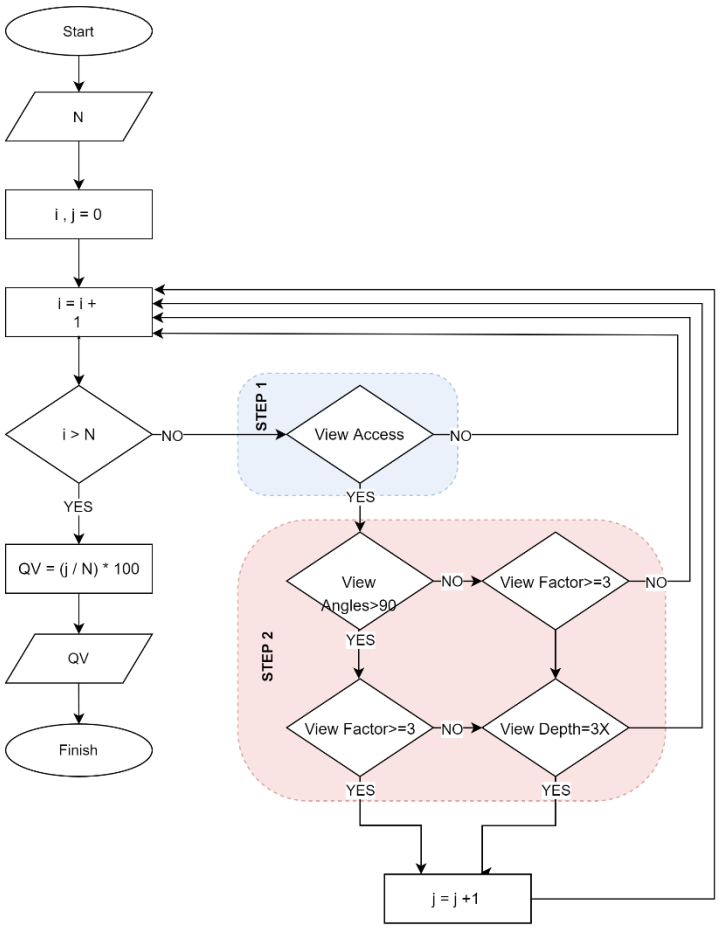

Figure 3- QV assessment flowchart for viewpoints. N is the number of viewpoints considered to study.

As discussed in Section 2.1, each view type must pass its own threshold. The minimum acceptable rate for the view access is 75% of all viewpoints. To pass the vertical and horizontal view angle evaluation, it should be more than 90 degrees for both angles. To achieve the VF of 3 or greater, both horizontal and vertical view angles should be more than 11 degrees. To pass the effective view depth evaluation, viewpoints should be located in a specific area near the window. In this area, the maximum distance of the viewpoints from the window could be three times the window head height. These thresholds are based on the LEED v.4 parameters to evaluate view to outdoor.

The view access is the percentage of the 360° horizontal view band visible from each viewpoint in the room (Figure 4, plan). This view type aim acknowledges the finding that a view to the outdoor is a highly valued quality of a window [90] and demonstrates the amount of regularly occupied spaces that has a direct line of sight to the outside.

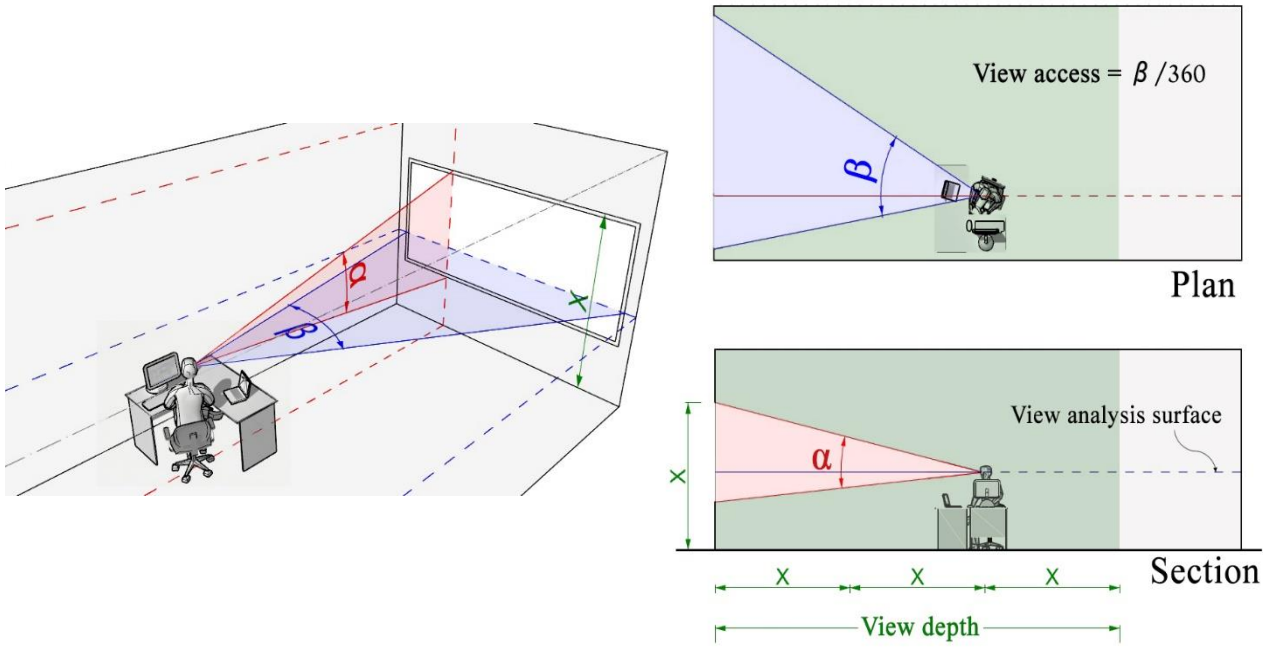

Figure 4- Illustration of studied parameters in QV evaluation. The α and β are the vertical and horizontal view angles respectively. The minumum α and β values are used to calculate the VF rating for each viewpoint. X is used to determine the view depth.

View angles are affected by the viewer's location, eye height and also the size and location of the window on the façade and affect the user's judgments of minimum acceptable window size [91]. In this study, the eye height of the viewer was set at 1.2 m above the floor as a seated observer [92] and horizontal and vertical angles for each point were defined, as illustrated in Figure 4.

The VF is based on a technical report of "Windows and Offices Report" [93], focusing on productivity in interior environments. The report presents the results of a statistical study into the relationship between the indoor office environment and worker performance. Having a high VF is strongly and positively correlated to having a 'large size window view', 'interesting' and/or a 'relaxing' view. The VF for each viewpoint is rated from 0 to 5 based on both view angles in Table 4. The minimum value of both vertical

angles (α) and horizontal angles (β) for each viewpoint were considered to modify VF. It is assumed that the views assessed in this study had no vegetation content.

Table 4- View Factor rating table based on both view angles. The smaller of the vertical and horizontal view angle values used to define the VF for each viewpoint.

View Factor	degrees
1	1-5
2	5-11
3	11-20
4	20-50
5	50-90

The largest VF rating of a 5 was defined as filling the seated observer's field of view. This was empirically determined to be at least a 50-degree viewing angle for both the vertical and horizontal view angles, which almost completely filled the visual field. Each subsequent lower category represented about one half of the previous angle.

Research shows that a view depth or user's distance from the window affects a viewer's judgment about the minimum width of an acceptable window [11] and also their satisfaction with the view [94] and comfort perception [13]. In this research, to have a QV according to LEED 4, viewer position should be located at a distance of 3 times the head height of the window. This distance actually defines the acceptable view depth in a room. In Figure 4, X is the distance to head-height of window and used to determine the view depth. View access is shown in the diagram as equal to 3X.

In this study, a grid size of 0.75 m was overlaid onto the view analysis surface, and 119 points were defined. Each view type evaluation and QV result (the area enclosed with a black line on view access analysis figure) was visualised in the upper part of each model diagram (Figure 9, 13 & 18).

3.5 Optimisation criteria

In the next step, the algorithm of location and dimensions of the window opening is defined, considering the limitations of the sill height and head height of 0.76 m and 2.28 m, respectively. The window parameters applied in this research are window width and height, window sill and head height and also distance of window edges from façade edges. The illustrated parameters in Figure 5 are described in table 5.

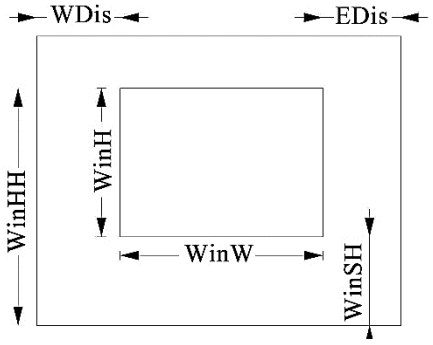

Figure 5-illustration of the research parameters.

These window parameters could change with an increase of 20 cm (table 5). With this method, more than 12,000 diverse openings in the range from 0.2 m to 1.52 m in height and 0.2 m to 3.60 m in width could be generated and evaluated. The largest possible window is also used as the base research model. An electrical load of 20.88 kWh/m^2 is considered for the equipment in all models; however, this load is removed from energy usage objective function, in order to achieve a better comparison.

Table 5- Research parameters detail and range.

Parameters	Description	Base model value	Lower limit	Upper limit	increment
		meters			
WinW	Window width	3.60	0.6	3.60	0.20
WinH	Window height	1.52	0.20	1.52	0.20
WinHH	Window head height	2.28	0.95	2.28	0.20
WinSH	Window sill height	0.76	0.76	1.71	0.20
WDis	Distance from the western edge of the window to the western wall	0.15	0.15	1.95	0.20
EDis	Distance from the eastern edge of the window to the eastern wall	0.15	0.15	1.95	0.20

3.6 Optimisation procedure

The overall procedure of optimising the window system is illustrated in Figure 6. When the simulation of the optimisation objectives is finished, the optimisation phase begins. In this phase, two processes are performed. In the first process, the research parameters are evaluated, by a back and forth process, ensuring a reasonable trade-off between the objectives (using Octopus software). Octopus settings are presented in Table 6. By producing different generations, the Pareto front is drawn and optimal solutions are extracted.

In the second process, after the end of the previous process, and not improving the overall optimisation result in the last generation in Octopus, the analysis of the research findings determines the optimum result. This is done by importing the parameters and objectives into the Excel, extracting the smallest values of objectives, then placed in applying the weighting fitness function. Using the fitness function presented in Section 3.3, the function value for each model is calculated, and the absolute optimum genome, as well as the fittest genomes in each objective, are found. The optimisation process took a week, on a desktop computer with Intel(R) Core(TM) i5-4460 CPU @3.20 GHz processor and 4.00 GB ram. During this optimisation process, about 2900 simulations were separately conducted for each objective, and 28 generations of genomes were produced. About 1500 generated models were duplicated and removed, so 1400 unique genomes were investigated.

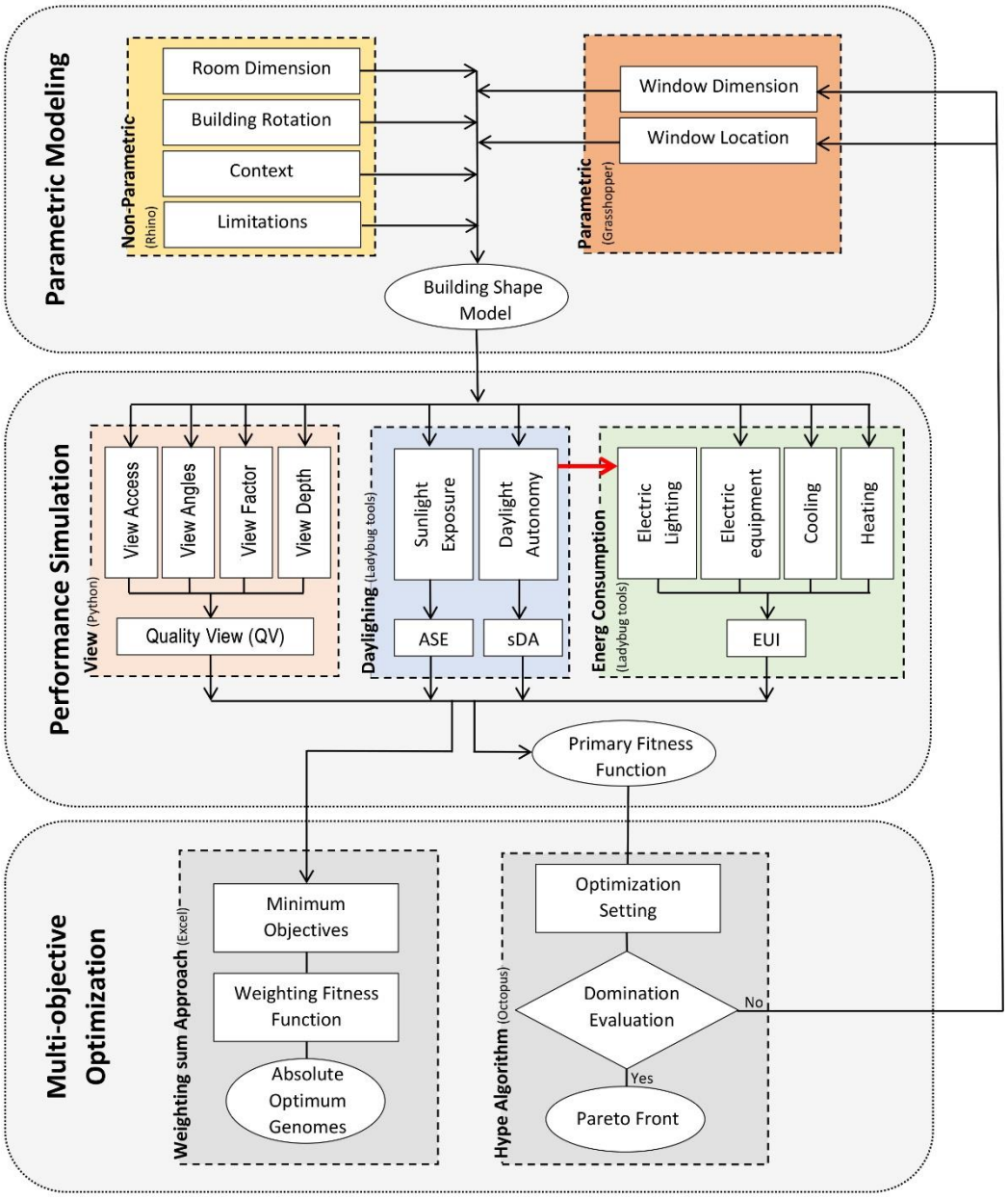

Figure 6- Research workflow. The red arrow in performance simulation is updated lighting schedule.

Table 6- Optimisation settings in Octopus.

Elitism	Mutation Probability	Mutation Rate	Crossover Rate	Population Size	Max Generation	Max Evaluation Time
0.5	0.1	0.5	0.8	100	None	None

3.7 Optimisation deviation

A similar method of calculating standard deviation is used to check the adequacy of the number of generations and iterations. In statistics, the standard deviation is a measure of the amount of variation or dispersion of a set of values. A low standard deviation indicates that the values tend to be close to the mean of the set, while a high standard deviation indicates that the values are spread out over a wider range.

In the proposed method of this research, the mean value is replaced by the value of the optimal absolute genome and the distance between the parameters/objectives and the optimal genome in each iteration is calculated.

The formula for the optimisation deviation is

$$\sigma_{opt} = \sqrt{\frac{\sum_{i=1}^{N}(x_i - x_{opt})^2}{N}} \tag{12}$$

where $\{x_1, x_2, \dots, x_n\}$ are the values of the parameters/objectives in a generation, x_{opt} is the value of the same parameter/objective in the absolute optimum genome, and *N* is the number of population in a studied generation.

The lower these values, the greater the convergence of the optimisation process. The results of these optimisation deviations (σ_{opt}) for each parameter or objective are shown in Table 7. The yellow highlighted numbers represent the least amount of distance from the optimal genome in different generations.

The lowest values tended to be obtained in the 23rd generation and the WDis values were carefully examined in the 28th generation. The trend line in Figure 7 shows that the distance between the WDis in each population with the optimal WDis has generally decreased compared to previous generations. Trend lines of other parameters/objectives also behave similarly to WDis. Since the lowest value for research optimisation deviation is reported in the 28th generation, the results of subsequent generations have not been reported.

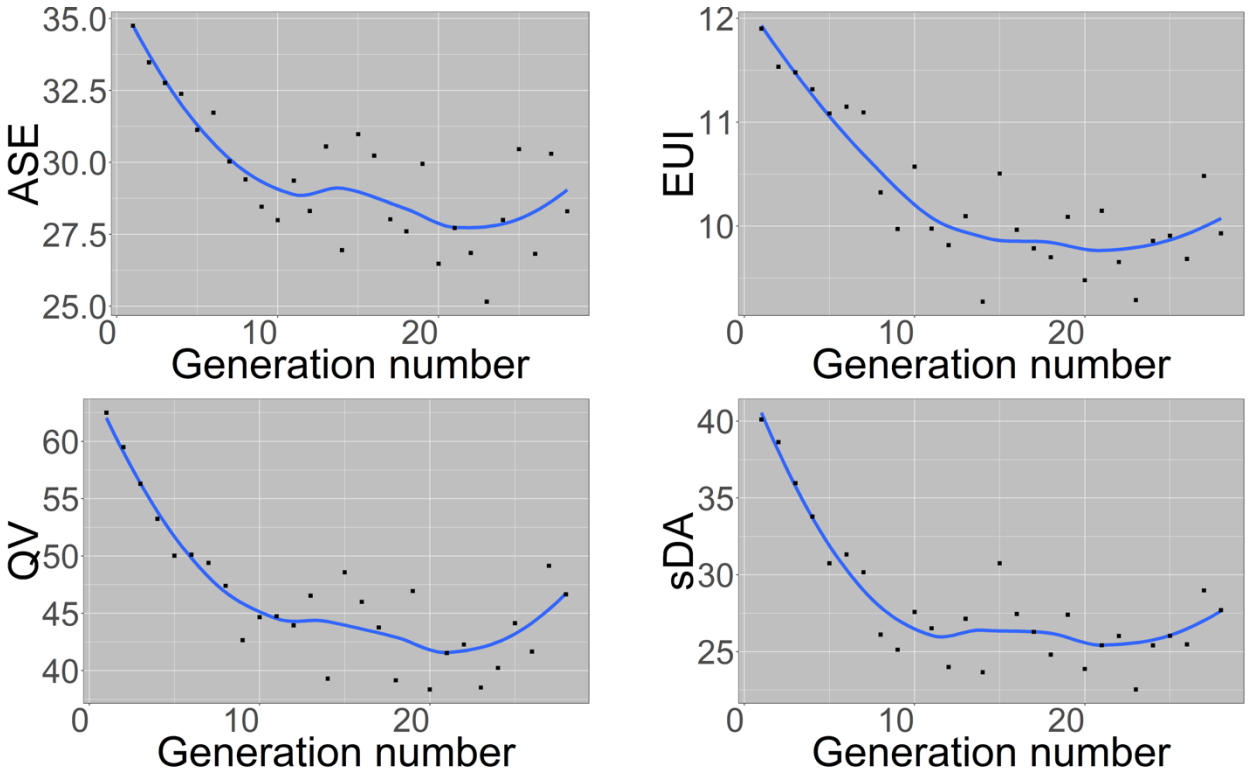

Figure 7- Results of σ_{opt} for research objectives in 28 generations. Downward trend line shows the convergence of the optimization process.

Table 7- Results of σ_{opt} for parametrs and objectives of 28 generations. Yellow highlighted have the least values in each column.

Optimisation generations	WinW	WinH	WWR	WinHH	WinSH	WDis	EDis	ASE	sDA	QV	EUI
G01	2.080	0.924	36.303	0.511	0.412	0.693	0.804	34.751	40.106	62.500	11.901
G02	2.046	0.866	35.134	0.420	0.446	0.760	0.810	33.475	38.630	59.493	11.534
G03	1.880	0.859	34.169	0.431	0.427	0.650	0.786	32.761	35.966	56.292	11.479
G04	1.774	0.807	32.940	0.334	0.473	0.714	0.736	32.383	33.788	53.233	11.317
G05	1.626	0.773	31.564	0.253	0.521	0.574	0.780	31.131	30.747	50.023	11.084
G06	1.618	0.771	31.821	0.249	0.522	0.630	0.820	31.727	31.326	50.107	11.149
G07	1.498	0.783	31.149	0.325	0.458	0.540	0.718	30.030	30.159	49.392	11.094
G08	1.310	0.768	29.140	0.285	0.483	0.542	0.536	29.408	26.108	47.393	10.323
G09	1.390	0.690	28.622	0.203	0.486	0.562	0.636	28.458	25.125	42.645	9.971
G10	1.516	0.693	29.722	0.260	0.433	0.518	0.742	27.988	27.579	44.661	10.572
G11	1.486	0.682	29.122	0.200	0.483	0.506	0.616	29.366	26.520	44.737	9.975

G12	1.344	0.695	28.166	0.182	0.513	0.530	0.602	28.307	23.999	43.939	9.815
G13	1.424	0.764	30.193	0.262	0.502	0.496	0.700	30.551	27.134	46.527	10.094
G14	1.362	0.610	27.223	0.173	0.437	0.478	0.716	26.946	23.654	39.292	9.271
G15	1.650	0.768	31.215	0.239	0.528	0.494	0.720	30.979	30.747	48.569	10.505
G16	1.492	0.747	29.992	0.217	0.530	0.500	0.696	30.231	27.453	45.997	9.963
G17	1.464	0.705	28.483	0.247	0.458	0.496	0.636	28.021	26.284	43.762	9.785
G18	1.464	0.617	28.003	0.160	0.458	0.586	0.602	27.601	24.806	39.149	9.699
G19	1.432	0.752	29.854	0.241	0.511	0.536	0.608	29.946	27.402	46.939	10.088
G20	1.426	0.598	27.214	0.198	0.401	0.518	0.716	26.475	23.873	38.351	9.478
G21	1.456	0.657	28.593	0.245	0.412	0.512	0.672	27.719	25.411	41.535	10.146
G22	1.452	0.680	28.546	0.184	0.496	0.540	0.688	26.853	26.015	42.275	9.653
G23	1.260	0.583	26.431	0.175	0.408	0.570	0.506	25.156	22.536	38.519	9.287
G24	1.514	0.610	28.638	0.182	0.427	0.568	0.606	27.996	25.402	40.233	9.857
G25	1.440	0.726	29.624	0.207	0.519	0.582	0.578	30.458	26.025	44.132	9.906
G26	1.376	0.673	27.996	0.228	0.445	0.574	0.602	26.820	25.470	41.653	9.683
G27	1.448	0.777	30.954	0.255	0.522	0.504	0.616	30.299	28.982	49.140	10.482
G28	1.456	0.709	29.411	0.236	0.473	0.460	0.600	28.299	27.696	46.653	9.929

4. Results

This section presents the results of parametric optimisation of daylight, energy, and view to outdoor. Initially, the base model for the optimisation algorithm is defined and the model simulation results are derived, for the purpose of comparison, with the recommended solutions from the proposed algorithm. The HypE algorithm mutates the model to create new generations, which are evaluated and returned to the optimisation algorithm. To find the most optimum solution, the weighted-sum function is introduced and ultimately, optimised solutions are introduced and discussed.

4.1. Base model simulation

According to the ASHRAE 90.1 standard [77], the maximum WWR is selected for the base model (Figure 8). Table 8 presents the detail of input parameters and calculated objectives.

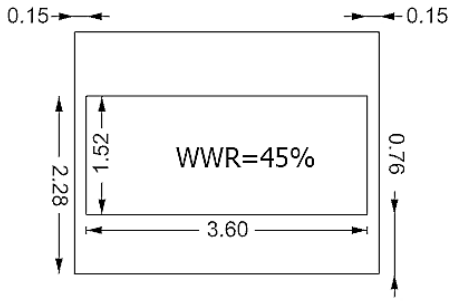

Figure 8- Base model elevation and parameters values.

Table 8- parameters and objective functions for the base case.

Model in optimisation process	Parameters						WWR	Objectives					Fitness Function
	WinW	WinH	WinHH	WinSH	WDis	EDis		ASE	sDA	DA_{swe}	QV	EUI	
	m	m	m	m	m	m	%	%	%	%	%	kWh/m^2	
Base	3.60	1.52	2.28	0.76	0.15	0.15	45.26	38.66	52.94	52.01	80.67	81.27	82.26

Figure 9 illustrates the view diagrams and monthly energy usage chart generated from Grasshopper. The large window size allows for sufficient light transmission to the interior to provide natural lighting. In this case, more than 50% of room space receives a mean of 300 lux, with daylight during the working hours throughout the year. On the other hand, aggregation of annual 250 hours of direct sunlight with 40% in the south face and the absence of a shading device, the base model fails to meet the minimum requirement set by the LEED v4.

View performance in the base model satisfied the proposed conditions, as all of the space has view access. Evaluation of view performance conditions reveals that 82% of the grid points are located at the distance of three times the window head height (view

depth), 15% are in a viewing angle of more than 90°, and the VF for 80% of them are more than three. Therefore, considering the majority of points that have passed the two out of three secondary conditions, 80% of the office room has satisfactory quality performance.

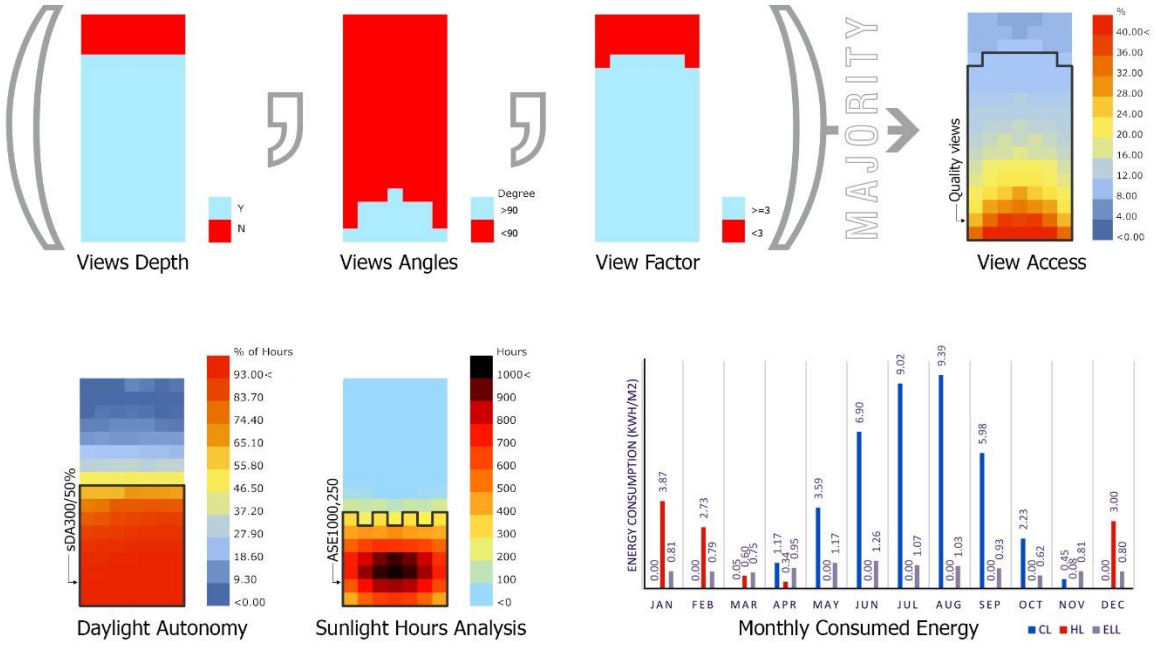

Figure 9- simulation results for the base case. Up: view analysis. Down: Daylight and energy consumption analysis.

The energy consumption for the base model is obtained, as 81.27 kWh/m^2. Figure 9 (down right), demonstrates the monthly distribution of EUI separated by the cooling, heating and electricity load. The cooling, heating and electrical lighting loads account for 48, 13 and 14 percent of total EUI, respectively. Accordingly, because Tehran is in a warm and dry climate, the priority of a design strategy should be to reduce the cooling load and preventing the sunlight penetration in summer.

4.2. Pareto frontiers solutions

Figure 10 illustrates the benchmarking Pareto fronts and the relationship between the four optimisation objectives. Due to a higher number of the objectives than the number of possible axes in a 3D chart, the fourth objective values (ASE) are demonstrated in the

blue-yellow colour spectrum. The optimisation algorithm explained in section 3.1 and also weighting sum approach in section 3.3, identified the yellow spheres as the most fitted solutions in the optimisation process. As it is demonstrated in Figure 10, while these spheres have the highest QV and sDA and the least EUI; their value of ASE are undesirably high. Although the optimization is set to reduce the value of ASE, this has led to considering the same weight for all objectives. There are other solutions with ASE less than 10% (section 5.4) which could be chosen in the proposed framework, but these models with low WWR, have lower performance in the other objectives. In addition, in the base model, no devices considered to control the glare. It seems that using glare control tools such as shadings can reduce ASE and increase the window size as long as performance improvement in other objectives.

Because it was difficult to understand the four-dimensional diagram, the values of the objectives were demonstrated and studied, in four 2D-dimensional diagrams in Figure 11. In this Figure, the base model is also shown as a green square, compared to other models. Besides, the top-ten genomes based on the fitness function, introduced in section 3-3, are highlighted. Their detailed characteristics are also presented in Table 9. Since the coordination centre point represents the best theoretical solution, the best solutions should be near the origin of the coordinates.

So each diagram has its own Pareto front and optimum genomes. In diagrams of 1, 2, 4 and 5 in Figure 11, the top ten optimum genomes are matched the optimum genomes of each diagram, but this is not in diagrams of 3, 6 and 7.

As the optimum genomes are introduced by the research optimisation algorithm, as mentioned earlier, the reason for high value of ASE in these models is the same weight of the research objectives. In addition, the formula 7 in section 3.3 also confirms the optimality of these models. In the top ten optimised models, the algebraic sum of the three values of sDA, EUI and QV has been so high relative to the other models that the effect of ASE has virtually disappeared. In this kind of circumstances, for having models with acceptable ASE values, models can be restricted to ASE less than 10%, or glare control tools be added to the research models configuration.

As shown in Figure 11, since the base model has the largest possible window, no further improvements in sDA nor QV in other genomes are found.

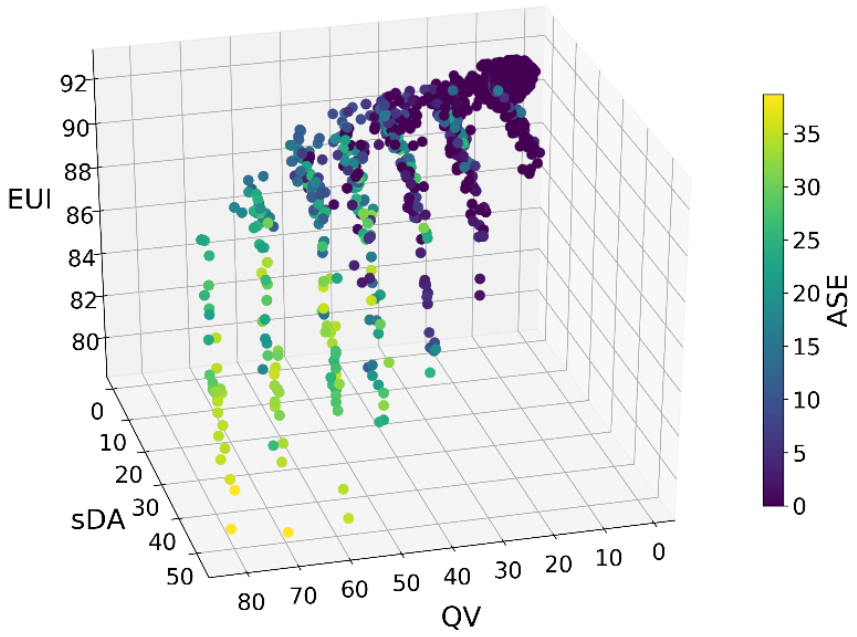

Figure 10- 4D chart of simulated models in optimization process. ASE values is illustrated by colour. The yellow spheres are elite-solutions.

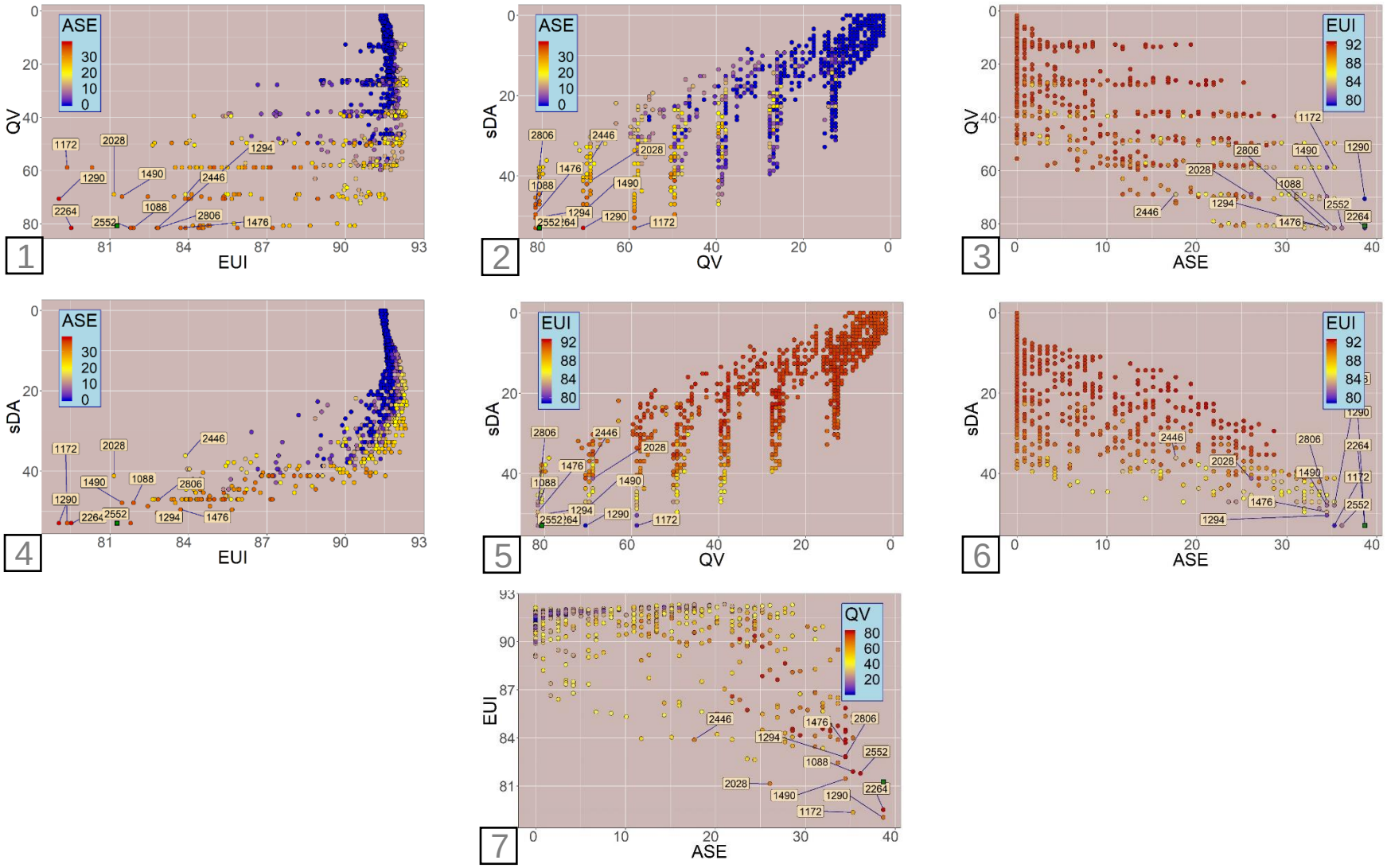

Figure 11- Genomes produced in Octopus. Normally the most optimum genomes are closest to the origin coordinates. Green point is the base model.

Because of the contradictory relationship between energy performance and view to outside, as well as energy and daylight, there are many genomes that show high performance in one objective, but not in others. When genome generations are produced, each generation contains genomes that are fitter than the genomes of previous generations. As shown in Table 8, the fitness function value for the base model was 82.26.

The best solution was found in the 22nd generation and its fitness function value represents the highest in this study, equal to 96.48. Its fitness function value improved by 3% compared to the base model. In later generations, no better genome was found, and the density of solutions increased in the range of origin of the coordinates. The number of generations of each of the top-ten solutions in which is produced is given in Table 9. For instance, the fifth and sixth solutions (genomes 1172 and 1088), produced in the 11th and 10th generations, and the genome 2806 produced in the 28th generation. Finding genomes with better fitness function continued until the 28th generation, and no better genome found in later generations. As such, although the optimisation for the further six generations continued, just the first 28 generations' results are reported in research.

Table 9- optimised genomes with their parameters and objective functions. The best single objective genomes among top-ten are highlighted and bordered with solid lines.

Model	Generation	Ranking	Parameters						WWR	Objectives				Fitness Function
			WinW	WinH	WinHH	WinSH	WDis	EDis		ASE	sDA	QV	EUI	
			m	m	m	m	m	m	%	%	%	%	kWh/m^2	
2264	22	1	3.40	1.52	2.28	0.76	0.35	0.15	42.75	38.66	52.94	81.51	79.52	96.48
1290	13	2	3.60	1.33	2.28	0.95	0.15	0.15	39.60	38.66	52.94	70.59	79.05	86.32
2552	25	3	3.20	1.52	2.28	0.76	0.15	0.55	40.23	36.13	52.94	81.51	81.79	85.91
2028	21	4	2.00	1.33	2.28	0.95	0.55	1.35	22.00	26.05	41.18	68.91	81.15	78.81
1172	12	5	3.60	1.14	2.28	1.14	0.15	0.15	33.95	35.29	52.94	58.82	79.36	77.93
1088	11	6	3.00	1.52	2.28	0.76	0.35	0.55	37.72	35.29	47.90	81.51	81.90	77.71
1294	13	6	3.00	1.52	2.28	0.76	0.55	0.35	37.72	35.29	47.90	81.51	81.90	77.71
2806	28	7	2.80	1.52	2.28	0.76	0.15	0.95	35.20	34.45	47.06	81.51	82.84	71.28
2446	24	8	1.60	1.33	2.28	0.95	0.75	1.55	17.60	17.65	36.13	68.91	83.88	70.49
1476	14	9	3.00	1.52	2.28	0.76	0.15	0.75	37.72	34.45	49.58	81.51	83.70	69.54
1490	15	10	3.00	1.33	2.28	0.95	0.35	0.15	33.00	34.45	47.90	69.75	81.46	68.46

In all 2910 generated models the minimum values, maximum values, average values and standard deviations of the total objectives are presented in Table 10. A lower standard deviation in EUI and ASE indicates that these objective values tend to be close to the average of their sets in the optimisation process, while a higher standard deviation in sDA and QV indicates that their values are spread out over a wider range. So the fitness difference among the optimised objectives and the rest of the models are suitably large.

Table 10- Objectives Information and Range.

	ASE (%)	sDA (%)	QV (%)	EUI (kWh/m^2)
Min	0.84	6.72	5.88	79.05
Max	38.66	52.94	81.51	92.34
average	5.80	17.13	24.14	90.91
Standard deviation	9.89	13.91	21.19	1.96

4.3. Optimised solutions

Table 9 shows the ten optimum solutions obtained as the Pareto front. Among all solutions, only the first three genomes have a fitness function value greater than the base model.

Because of the antagonistic relation among sDA and EUI or QV and EUI, many solutions are found that consume more energy, while receiving less daylight. These solutions share similar parameters as demonstrated in Table 11. These similarities include low WWR, an aspect ratio of 3:1 to 6:1 and the lowest possible position of the window. Due to low WinHH in these models, on average only 22% of the room receives enough light in 50% of the occupied hours in a year, and more than 20% of the room receives more than 1,000 lux over 250 hours per annum. In addition, the low position of the window, in spite of the high aspect ratio, restricts the view to the sky comparing to the base model. To investigate the cause of increases in EUI, the model 1524 was compared to the base model. Table 12 shows a significant increase of more than 130% in the electric lighting energy consumption, whilst it's cooling, and heating load only decreased by 9% and increased by 1.5%, respectively. Thereby, the lack of sufficient daylight in this model leads to an increase in electrical lighting load and subsequently, a higher total energy consumption.

On the other hand, there are solutions posing higher sDA and QV values but less energy usage, such as solutions 2264, 1290 and 2552 (Table 12). The main difference between models having high EUI and lower sDA and QV, is the larger WWR, about 40% on average. The WinHH is maximum so that the daylight penetration and view to the outside are increased, and the WinSH is enlarged to 1.5 meters to reduce the possibility of sunlight penetration.

Table 11- Genomes with highest EUI and lowest sDA & QV: parameters, objectives and fitness values.

Model	Parameters						WWR	Objectives				Fitness Function
	WinW	WinH	WinHH	WinSH	WDis	EDis		ASE	sDA	QV	EUI	
	m	m	m	m	m	m	%	%	%	%	kWh/m^2	
1524	3.00	0.57	1.33	0.76	0.35	0.55	14.14	21.01	23.53	27.73	92.34	-77.27
1771	3.00	0.57	1.33	0.76	0.15	0.75	14.14	21.01	22.69	26.05	92.33	-80.90
873	2.60	0.57	1.33	0.76	0.15	1.15	12.26	17.65	19.33	26.05	92.32	-78.49
1599	2.00	0.76	1.52	0.76	0.55	1.35	12.57	15.97	19.33	37.82	92.31	-59.28
1006	3.00	0.76	1.52	0.76	0.55	0.35	18.86	28.57	29.41	39.50	92.30	-70.69

Table 12- Energy consumption comparison among some selected models and the base model.

Model	Cooling Load	Heating Load	Electrical Lighting Load	Electrical Equipment Load	Total Thermal Load
	kWh/m^2				
1524	35.29 ↓	10.79 ↑	25.39 ↑	20.88	92.34 ↑
Base model	38.78	10.63	10.99	20.88	81.26
2264	36.37 ↑	10.86 ↑	11.41 ↑	20.88	79.52 ↓
2264-mirrored	↑ 39.20	↓ 10.60	↑ 12.37	20.88	↑ 83.04
1290	↓ 35.92	↑ 11.11	↑ 11.14	20.88	79.05↓

5. Selection of the Best Model

In this section, the selection of the best models, based on the different objectives are elaborated. A comparison between the Pareto front solutions is performed, with the base

research model, to show how different parameters affect building performance, and what effect this has on improving the efficiency of the genomes.

5.1. The best optimum genomes

The best optimum solution at the Pareto front is defined as a balance between daylight performance, energy consumption, and QV. The best fitness value is achieved for the model 2264 (Figure 12), by 96.47. The energy consumption of the model is 79.52 Kwh/m^2 with 2% reduction compared to the base model. The annual energy distribution is shown for the best optimum model, on the right-hand side of Figure 13. Because of the lower WWR than the base model, the penetration of the solar radiation and the adequate distribution of natural light is decreased, which results in a 2.16, and 4% increase in heating and electrical light loads and a 6.62% reduction in cooling load (Table 12). However, due to the nature of Tehran's hot climate, the total energy consumption is decreased.

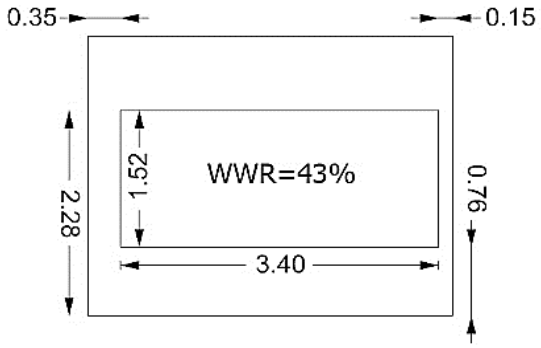

Figure 12- absolute optimum genome elevation and parameters values

The daylight simulation of the best optimum genome in the bottom left-hand side of Figure 13 shows that the sDA and ASE are the same as the based model with values of 52.94 and 38.66, respectively. For better comparison, DA_{ave} was calculated, given that the sDA is a spatial index and does not give information about light distribution (Table 13). In the optimum model, DA_{ave} falls 2% (50.88%), which means that, in less than 2% of occupancy hours, there was less daylighting. Due to the smaller WWR, this decrease seems natural and justifies the increase in electric lighting consumption.

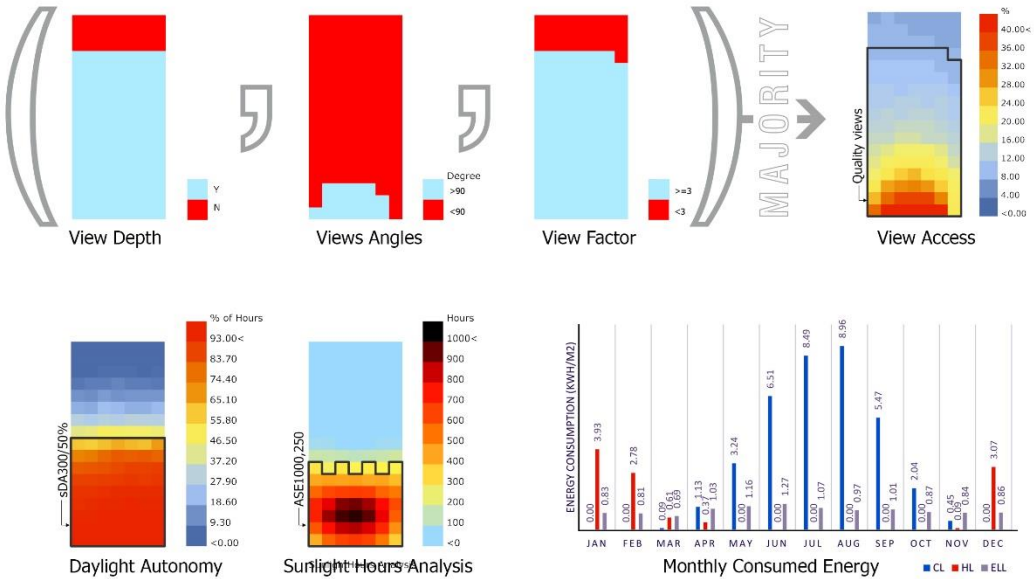

Figure 13- simulation results for the absolute optimum genome. Up: view analysis. Down: Day light and energy analysis.

In the best optimum genome, 81% of the points in the office room have quality views, which is 1% higher than the base model. By comparing the analysis of the three conditions of QV in Figures 12 and 9 it is revealed that in both models there are limited points that had a view angles of 90 degrees or more. In addition, the points that located in the distance of three times, the WHH were the same. Therefore, an effective factor, which led to a difference in QV between the two models is the VF.

To analyse the effect of EDis and WDis, on the best optimum genome, a new mirrored model was generated, with the reverse dimensions. This model is not among the Pareto front solutions and consequently, it is individually simulated. The result of this simulation (presented in Table 13) indicates that these two models are similar, in terms of ASE, sDA, and QV, and they deviate only in EUI and DA_{ave} values. In the mirrored model, the DA_{ave} dropped by only 0.08%, yet its electric lighting load increased by 8%. The heating load in this model decreased by 2% and the cooling load increased by 7%. As mentioned earlier, due to the greater sensitivity of the cooling load, the total energy consumption increased by about 4%. For this reason, it was concluded that in a window of a specific size, it is likely to be better to place a window near the eastern wall in this research climate.

Table 13- Parameters and objectives of the absolute optimum genome.

Model in the optimisation process	Total optimum genome	Parameters						WWR	Objectives					Fitness Function
		WinW	WinH	WinHH	WinSH	WDis	EDis		ASE	sDA	DA_{ave}	QV	EUI	
		m	m	m	m	m	m	%	%	%	%	%	kWh/m^2	
2264	1	3.40	1.52	2.28	0.76	0.35	0.15	42.75	38.66	52.94	50.88	81.51	79.52	96.47
mirrored-2264	-					0.15	0.35				50.80		83.04	69.94

5.2. The energy optimum model

Figure 14 shows the optimum energy consumption genome (model 1290). This model holds the same sDA and ASE as the best optimum model and the base model, however, in terms of DA_{avg} value, it stands between those two models (Table 14). Since the WWR is smaller than theirs, the DA_{avg} is 0.83% lower than the base model, nevertheless, as a result of the lower EDis as well as its symmetry, light distribution is more uniform and about 0.3% higher than the best optimum model.

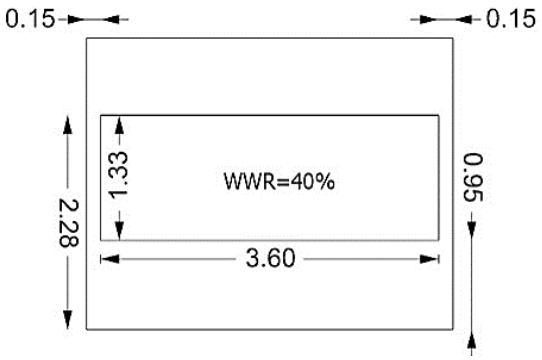

Figure 14- Energy optimom genome elevation and parameters values

QV in the optimum energy model is also 2.7% and 4.8% less than the base and best optimum models, due to the reduced WinSH and VF. The energy optimum genome shows 7.4% and 1.2% decline in cooling load, in comparison to the base and the best models, respectively; and 4.5% and 2.3% increase in heating loads. Furthermore, as a result of the reduction in WWR (by 5.7% and 2.7%, against the base and the best optimal models), the possibility of solar radiation penetration in the summer and winter declined, which justifies those changes in thermal loads. At the same time, the interstitial state of this

model in daylight, relatively to the base and the best optimal models, has a consistent effect on the lighting energy consumption, and its electrical load is 1.4% higher than the base and 2.4% lower than the best optimal model (Table 14). Although this model has a higher heating load than the other two, and the corresponding electrical lighting load is larger than the base model, the impact of the cooling load on the energy consumption is higher; and accordingly, the total energy consumption is lower.

Table 14 -Parameters and objectives of the energy optimum genome .

Model in the optimisation process	Total optimum genome	Parameters						WWR	Objectives					Fitness Function
		WinW	WinH	WinHH	WinSH	WDis	EDis		ASE	sDA	DA_{ave}	QV	EUI	
		m	m	m	m	m	m	%	%	%	%	%	kWh/m^2	
1290	2	3.60	1.33	2.28	0.95	0.15	0.15	39.60	38.66	52.94	51.18	70.59	79.05	86.32

5.3. The best sDA genome

Amongst the 2910 models investigated in the optimisation process, four models were found fitter than the others (Figure 15). These four models had equally the highest sDA values (52.9%). The average sDA is 29.5% with a standard deviation of 13.91 (table 10), so the sDA values are spread out over an acceptable range. Parameters and objectives of some randomly generated models are presented in Table A.1.

In these models, possessing different parameters, almost 53% of the room has enough daylight at all occupied hours. These genomes are among the top-5 solutions, with the highest fitness function value.

The models in which the sDA value is maximised represent the three highest possible values for WinH and WinW. DA_{avg} is calculated for comparison of the options. As shown in Table 15, Model 1290, which is the second optimum model, has the highest average annual gain (more than 300 lux), which is 0.83% lower than the base model.

It is perceived that the high WinW and the symmetry of the model result in gaining more daylight than the models 2264 and 2552. In addition, model 1290 has a better fitness function than model 1172, due to the lower WinSH and the higher WinH. Figure 15, also

illustrates the higher brightness of the back position of the room, in this model, in comparison with other models. In the last row of the grid, there are points that in 9-27% of the year had daylight more than 300 lux. Such points are rare in the best optimal model and do not exist in models 2552 and 1172.

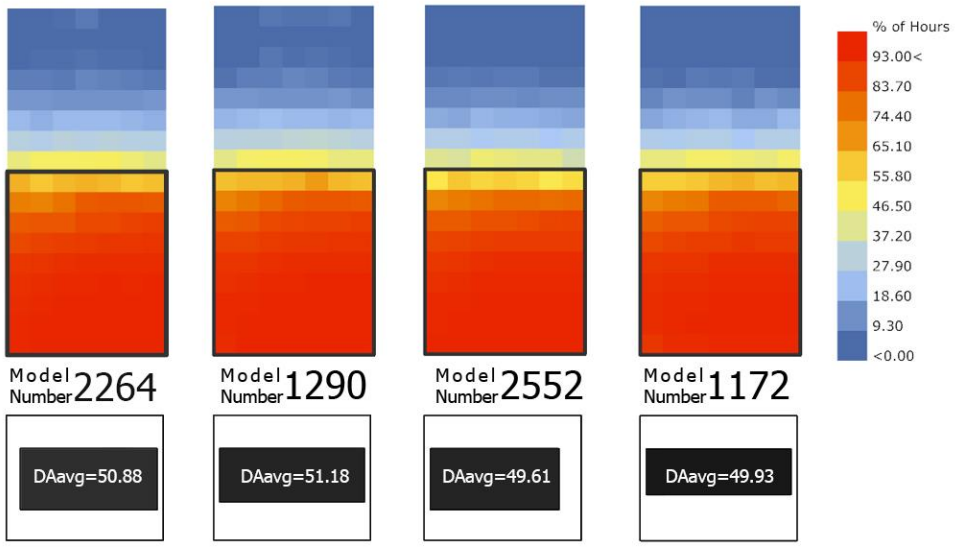

Figure 15-Daylight Autonomy in optimum genumes of SDA. Model 1290 has the highest DAavg. Areas with $sDA_{300/50\%}$ is demonstrated by black lines. The back of the room is brighter in model 1290 than others.

None of the four fitting models, having the best sDA, as well as the base model (with the largest possible WWR and sDA=52.94%) meet the LEED needs. As the sDA has a spatial definition, one of the ways to qualify for its LEED point, is reducing the depth of the room. Calculations show that if the simulated room has a maximum of 5.8 meters depth, the maximum points in daylighting is attainable.

Table 15- Parameters and objectives of sDA optimum genome

Model in the optimisation process	Total optimum genome	Parameters						WWR	Objectives					Fitness Function
		WinW	WinH	WinHH	WinSH	WDis	EDis		ASE	sDA	DA_{ave}	QV	EUI	
		m	m	m	m	m	m	%	%	%	%	%	kWh/m^2	
2264	1	3.40	1.52	2.28	0.76	0.35	0.15	42.75	38.66	52.94	50.88	81.51	79.52	96.47
1290	2	3.60	1.33	2.28	0.95	0.15	0.15	39.60	38.66	52.94	51.18	70.59	79.05	86.32
2552	3	3.20	1.52	2.28	0.76	0.15	0.55	40.23	36.13	52.94	49.61	81.51	81.79	85.91
1172	5	3.60	1.14	2.28	1.14	0.15	0.15	33.95	35.29	52.94	49.93	58.82	79.36	77.93

5.4. The best ASE genome

As stated in the literature review, less than 10% of the work plane should have more than 250 hours of direct sunlight in excess of 1,000 lux, in order to meet the LEED requirements. Among the generated models, 1033 models met these specifications. This was reduced further as 107 models (with average WWR of 1.22%), in which sDA is equal to zero, were removed. Among the remaining solutions, the model 2154 with ASE of 8.40, achieved the highest fitness function value. Whilst there were ten models with higher ASE (9.24), these had lower fitness function values.

Among these top-ten models, model 723 scored the highest fitness function of 10.79. Among the models with the lowest ASE (zero), the model 2426 has the highest fitness function of 28.99. In the top-ten genomes, the model 2446 with the fitness function of 70.49 had the best ASE with 17.65% (Table 16). Figure 16 shows a comparison between the ASE of all these models.

Model 723 and 2426 both have the same WinW, WinH, WWR, and location. However, higher WinSH and lower WinHH in model 723, cause a reduction in ASE. It is observed that the high WinW of the model 2154, the decrease in the WinSH, and the increase in the WinHH of the model 2446, lead to an increase in ASE. Comparison of model 2154 (the ASE optimum model with ASE less than 10% and the highest fitness function) with other models show that if high WinW is recommended (to improve other objective function values), it increased WinSH can reduce solar penetration and glare.

There are 707 models with zero ASE among the investigated models. The standard deviation for WinW, WinH, WinHH and WinSH parameters of these models are 0.8, 0.3, 0.4 and 0.3, respectively. Given that the lower the standard deviation, the less dispersion of data, so it indicates the high impact of architectural design parameters on the loss of glare.

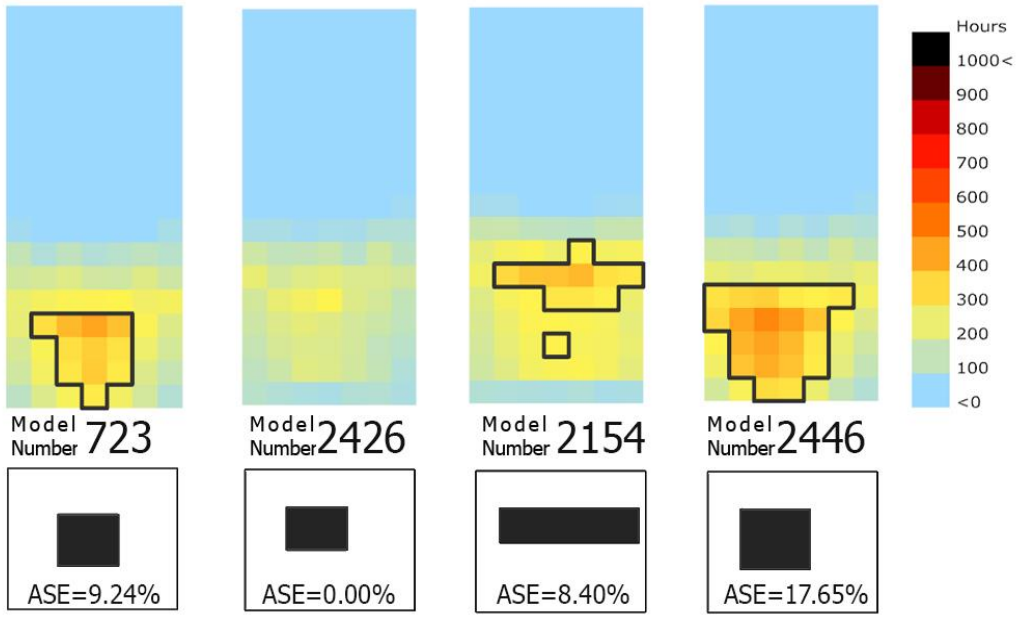

Figure 16- sunlight hour analysis of the best ASE optimum genomes. Areas with ASE more than 250 hour with more than1000 lux annually is demonstrated by black lines.

Table 16- Parameters and objectives of ASE optimum genomes

Model in the	Total optimum	Parameters	WWR	Objectives	Fitness Function

		WinW	WinH	WinHH	WinSH	WDis	EDis		ASE	sDA	DA_{avg}	QV	EUI	
		m	m	m	m	m	m	%	%	%	%	%	kWh/m2	
2446	8	1.60	1.33	2.28	0.95	0.75	1.55	17.60	17.65	36.13	NA	68.91	83.88	70.49
2154	1250	3.20	0.76	2.28	1.52	0.55	0.15	20.12	8.40	44.54	NA	38.66	85.53	59.96
2426	22	1.40	0.95	2.28	1.33	0.95	1.55	11.00	0.00	29.41	27.43	49.58	90.55	28.99
723	92	1.40	1.14	2.09	0.95	1.15	1.35	13.20	9.24	30.25	NA	57.14	91.26	10.79

Figure 17 shows the optimum ASE genome. Model 2426, has the rank of 22nd in the list of the best genome. Although this genome was less likely to have glare than the absolute optimal genome, it still did not receive enough daylight in 24% of the room, and 32% of the rooms had no QV (a major change occurred in VF), as well as 14% more energy consumption (Figure 18). Due to the smaller WWR, the cooling load decreased by 12% and 6%, relative to the basic model and the absolute optimum.

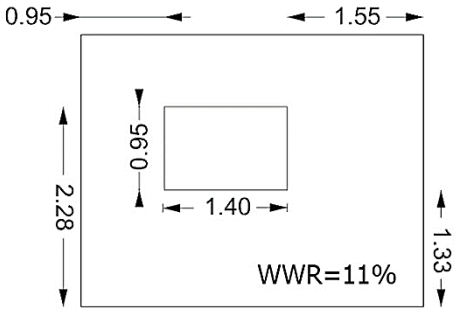

Figure 17- Annual sunlight exposure optimom genome elevation and parameters values

In winter, due to the decrease in received solar radiation, the heating load increased by 11% and 9%, relative to the basic model and absolute optimum. In this model, due to

reduced daylight, the electrical lighting load doubled (116% and 112%, respectively, relative to the absolute optimal model and base model).

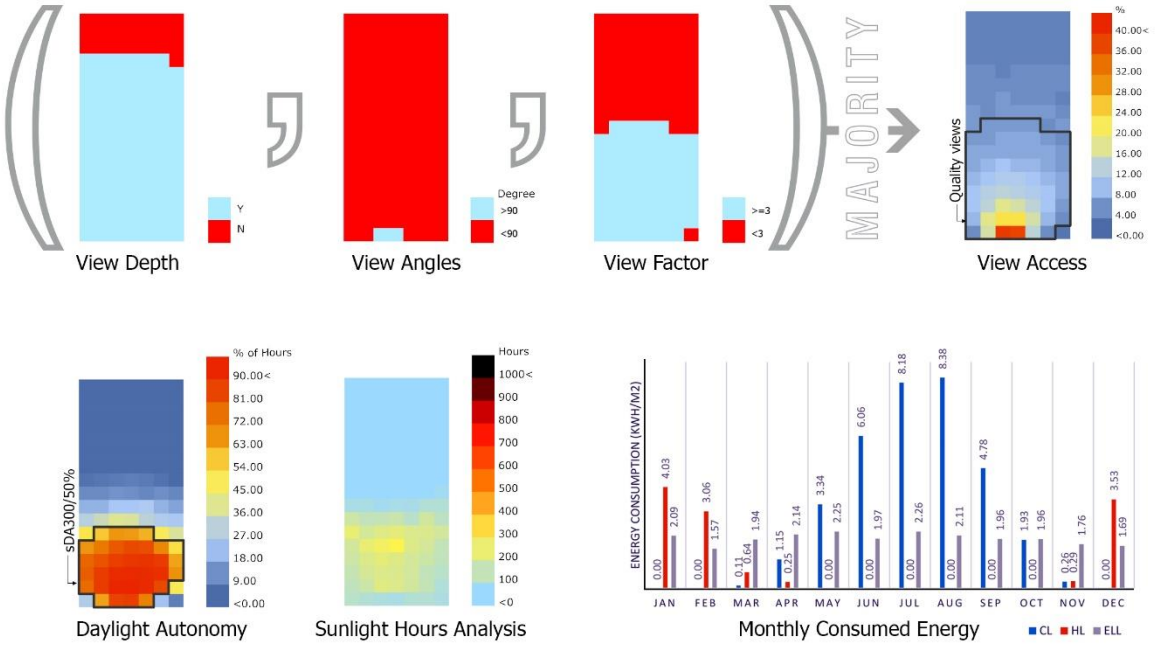

Figure 18- Simulation results for the annual sunlight exposure optimum genome. Above: view analysis. In view access analysis figure, areas with QV is demonstrated by black lines. Below: Daylight and energy analysis. In daylight autonomy figure, areas with $sDA_{300/50\%}$ is demonstrated by black lines. There is no area in "sunlight hours analysis" figure which have more sunlight more than than 250 hours.

5.5. The best quality views genomes

In all solutions, 14 models have the highest QV of 82%, which are more than 1% higher than the base model. To find the QV optimum model, more accurate simulations are performed by having the grid size and doubling the grid points (Table 17). The comparison shows that among parameters, just the view angles are effective, and the other parameters have constant values. Although the view angles do not influence the final outcome of the QV in this study, it helps to determine the optimum QV genome among those 14 models.

Table 17- view simulation results with a smaller grid size. The 5 best view genomes of table 15 and also the base model are comparable.

Model in the optimisation process	View depth	View angles	VF >= 3	View access	QV
2264	79.41	13.73	80.98	100.00	79.41
2552	79.41	11.76	80.78	100.00	79.41
Base	79.41	15.10	80.78	100.00	79.41
2806	79.41	9.02	80.39	100.00	78.82
1476	79.41	10.59	80.39	100.00	79.02
1060	79.41	7.84	80.20	100.00	78.82

The view angles are the same for some models due to the fixed WinW, WinH and changing WDis and EDis. Naturally, this change, regardless of the view content, should have an impact on the view to outdoor. 13% of the room in model 2264 and 2552 had more than 90˚ horizontal and vertical view angles. These models were the first and third best ranks of the optimum QV solutions.

In all of these 14 solutions, the WinW, WinHH, and WinSH were fixed, and just WinW, WDis, and EDis were changing. The WinSH and WinHH had minimum and maximum possible values, respectively, and therefore, the WinH had the highest possible value. By decreasing the WinW, the number of points in a room, with view angles of more than 90˚, decreased.

Although the model 2264 differed in WinW from the model 2552, the number of points obtained with the view angles of more than 90˚ were the same for both models. To better understand the reasoning behind this, the grid size was reduced to half the size (0.25 m), and the simulation was rerun for these models. With a smaller grid and more precise simulation, it was clear that the model 2264 had approximately 2% more points with view angles of more than 90˚, and approximately 1% had a VF value greater than 3. As shown in Figure 19, the points at the room end in model 2552 had less view access.

Results of simulation with a precise grid size in Table 18 showed that the two optimum models of 2264 and 2552 had the same QV. The view angles reduced with a drop in WinW, resulting in lower view angles compared to the base model. The model 2264 had the highest VF among the three models. Consequently, since the base model had the

maximum possible QV, during the optimisation process this value remains constant and it attempts to stabilise its other improved objectives.

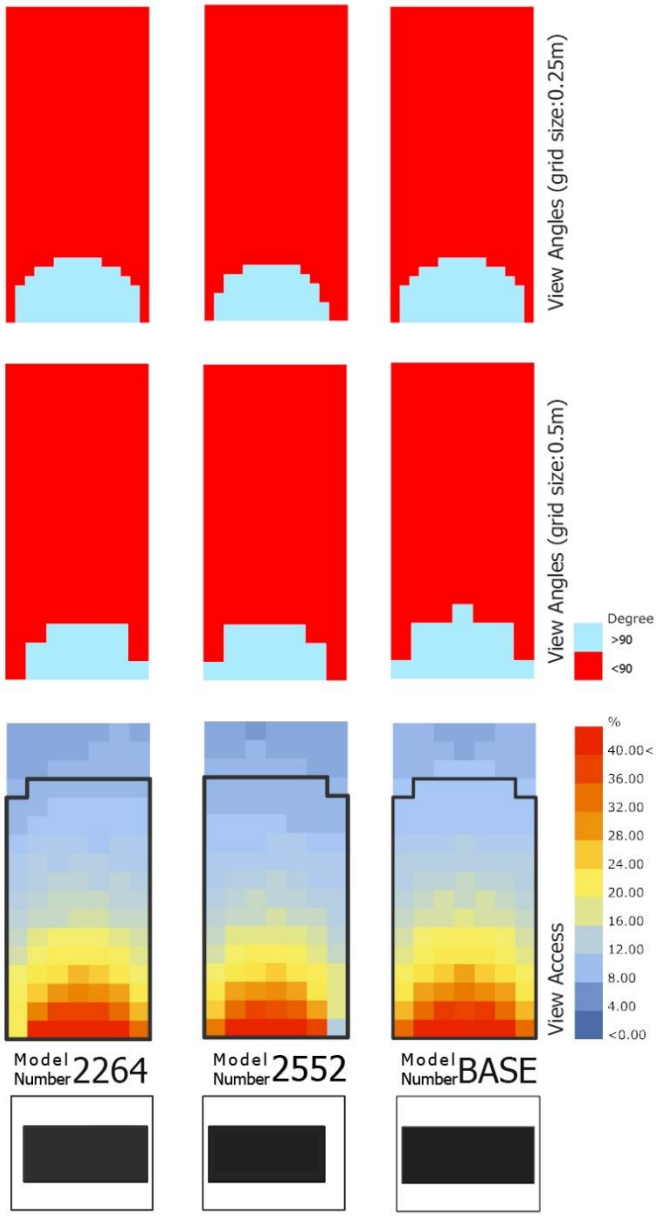

Figure 19- View comparison among the optimum view genomes and base model. Down: view access. The points with quality views are demonstrated by black line. Middle: view angles analysis with default grid size. Up: view angles analysis with smaller grid size.

Table 18- Parameters and objectives of view optimum genomes.

Model in optimisation process	Total optimum genome	Parameters						WWR	Objectives								Fitness Function
									Daylight		Quality View					EUI	
		WinW	WinH	WinHH	WinSH	WDis	EDis		ASE	sDA	View depth = 3X	View angles > 90	View factor >= 3	View access	Majority		
		m	m	m	m	m	m	%	%	%	%	%	%	%	%	kWh/m$_2$	
2264	1	3.40	1.52	2.28	0.76	0.35	0.15	42.75	38.66	52.94	82.35	12.61	81.51	100	81.51	79.52	96.48
2552	3	3.20	1.52	2.28	0.76	0.15	0.55	40.23	36.13	52.94	82.35	12.61	81.51	100	81.51	81.79	85.91
2806	8	2.80	1.52	2.28	0.76	0.15	0.95	35.20	34.45	47.06	82.35	9.24	81.51	100	81.51	82.84	71.28
1476	10	3.00	1.52	2.28	0.76	0.15	0.75	37.72	34.45	49.58	82.35	10.92	81.51	100	81.51	83.70	69.54
1060	17	2.60	1.52	2.28	0.76	0.35	0.95	32.69	34.45	47.06	82.35	8.40	81.51	100	81.51	83.89	63.36
1787	17	2.20	1.52	2.28	0.76	0.75	0.95	27.66	31.93	45.38	82.35	5.88	81.51	100	81.51	84.57	61.62
2859	18	2.20	1.52	2.28	0.76	0.95	0.75	27.66	31.93	45.38	82.35	5.88	81.51	100	81.51	84.57	61.62
1975	25	2.60	1.52	2.28	0.76	0.95	0.35	32.69	34.45	47.06	82.35	8.40	81.51	100	81.51	84.39	59.59
276	27	2.80	1.52	2.28	0.76	0.75	0.35	35.20	34.45	47.06	82.35	9.24	81.51	100	81.51	84.51	58.70
1201	28	2.80	1.52	2.28	0.76	0.35	0.75	35.20	34.45	47.06	82.35	9.24	81.51	100	81.51	84.51	58.70
1422	62	2.40	1.52	2.28	0.76	0.55	0.95	30.17	34.45	47.06	82.35	6.72	81.51	100	81.51	85.87	48.44
591	87	2.60	1.52	2.28	0.76	0.55	0.75	32.69	34.45	47.06	82.35	8.40	81.51	100	81.51	87.21	38.37
1294	6	3.00	1.52	2.28	0.76	0.35	0.55	37.72	34.45	50.42	82.35	10.92	81.51	100	81.51	82.80	77.90
1088	7	3.00	1.52	2.28	0.76	0.55	0.35	37.72	35.29	47.90	82.35	10.92	81.51	100	81.51	81.90	77.72

5.6. Improvement in the optimisation process

In this section, the objective results of the best optimum genome are compared with the objective results of the base model and the objective average values to demonstrate the improvement in the optimisation process and also to evaluate meeting the requirement of LEED rating system.

The average QV of the studied models is 24.14% (Table 10). This objective was significantly improved in the best optimum genome (81.51%; Table 9). Thus, the QV in the optimal model is more than 2.3 times higher than the average which also meets the view requirements specified in LEED. The QV in the optimum genome is increased by about 1% in comparison to the base model.

Energy consumption of the studied models has the lowest standard deviation among other objectives (Table 10). It represents that the difference between the minimum and maximum EUI is just 13 kWh/m^2/y. Although with the average EUI of 90.91 kWh/m^2/y, these low differences could not make a difference in meeting the LEED requirements, in the optimisation process, EUI in the optimum genome is decreased by about 2% in comparison to the base model.

Although both daylight indices rose significantly compared to an average of themselves, there is no significant change in these indices compared to the base model. sDA in the optimum genome (52.94%) increased more than 2 times than the sDA average value (17.13%), therefore, the chance of getting the minimum score of daylighting in LEED has increased. ASE value in the best optimum genome (38.66%) is equal to the highest found values, more than 5 times higher than the average.

Given that the ASE average value (5.80%) is less than 10%, it is apparent that the optimisation process has reduced the amount of this objective to meet the needs of the LEED. However, since the weight of each objective in the method used in Section 3.3 was the same for all the objectives of this study, the found best optimum genome with the highest fitness function has no acceptable ASE value. The authors suggest that in such projects, in order to find models that can meet LEED requirements in the daylighting alongside the other objectives, the weight of the ASE in Formula 7 should be increased.

Because of the relatively large size of the window used in the base model, the optimisation process did not change the LEED credits of this specific model. However, the model's ability to maintain the positive aspects of a larger window while reducing the negative impacts, are clearly observable. With no change in daylighting, the best optimum genome has a more quality view and consumes less energy than the base model. Certainly, a greater impact on the result of the optimisation could be achieved by choosing a smaller base model.

6. Conclusion

The research presented in this paper addresses the theoretical and methodological gap in configuring window systems for the design of office buildings. The design of window systems directly affect aspects of a building's quality and performance, including building energy performance, daylight gain, and visual comfort. As is evident in the reviewed literature, a reliable method for assessment of the Quality of View (QV) has not been introduced. The evidence on optimisation of window system design has focused on energy performance and daylight aspects of windows. The few studies concentrating on outside view tended to present qualitative methods to maximise WWR. This paper developed a framework for quantitative evaluation of QV by considering several factors including view access, view angles, VF and view depth.

This framework provides a foundation method to evaluate the QV for office environments. A multi-objective optimisation method was also introduced in this research design as a decision-making tool to assist building designers and engineers to achieve an optimised window system. This tool considers three optimisation objectives, namely: energy usage, received daylight and quality of view. The aim was to minimise energy usage while maximising received daylight and quality of view. The optimisation framework utilised Rhinoceros software for modelling the building, Grasshopper environment with two plugins (Ladybug and Honeybee) to calculate the energy usage and daylight and a Python-based plugin to evaluate the QV. The optimisation algorithm (HypE), which is a hypervolume-based evolutionary algorithm, is applied using Octopus (a Grasshopper plugin).

The optimisation operation was applied to a case study, which was a reference room in an office building based on a room specification defined for standardizing dynamic evaluations in office environments [87]. After validating the energy and daylighting simulation results with that specified room (Reinhart reference room), the location changed to Tehran city, Iran. The results of the proposed optimisation procedure were provided as a set of optimum solutions. Further to the obtained values for the optimisation objectives, a fitness function was introduced to better evaluate the performance of each configuration by weighting different objectives. The solution packages provide the decision-makers with potential options to select based on their expectations. The optimisation results showed that the suggested research framework can improve the daylighting and QV results more than times in comparison to theses average optimisation values. As for the EUI, this improvement was about 12%. The optimum solutions proved the efficiency of the optimisation framework in finding the best window system, for satisfying all studied objectives. It was revealed that it is possible to provide a satisfactory QV performance, for more than 80 percent of the reference room points, while minimising the energy usage, and maximising the daylight.

It was determined that in order to meet official standards set for office buildings as they relate to view, room geometry must be within the set of optimisation variables. The low complexity of the reference building may introduce other difficulties in satisfying the predefined standards. Similarly, additional building elements such as blinds, shades, and glazing play a role in controlling solar radiation, light amounts, and glare and therefore must be considered.

There is an opportunity for further studies to investigate the impact of shading and light control strategies on the studied optimisation objectives. Adding shading devices to facades provides an opportunity for simultaneous reduction in radiation transmission and heat gain energies, as well as a higher capability of controlling day-lighting [95]. However, the effects of such devices (e.g. blinds, screens, and shutters to the glazed surfaces, as well as implementing control strategies) on the quality of the view to outside have been under-researched.

Future research could also explore variations in the external environment of the building and to understand the resulting impact on the triple analysis of daylight, visibility, and energy. The view indices examined in this research design were internal, and external indices such as view content and external distance haven't been considered in the presented study in this paper. In future research, these could be considered when assessing the quality of view and result in more precise contextual results.

References

[1] Energy USDO, US Energy Information Administration, US Department of Energy, United States Government Printing Office: Washington, DC, 2013. Last Access: 28/10/2019

[2] Mhalas A, Kassem M, Crosbie T, Dawood N, A visual energy performance assessment and decision support tool for dwellings, Visualization in Engineering 1 (1) (2013) 7. doi: https://doi.org/10.1186/2213-7459-1-7

[3] Mahdavinejad MJ, Matoor S, Feyzmand N, Doroodgar A, Horizontal Distribution of Illuminance with Reference to Window Wall Ratio (WWR) in Office Buildings in Hot and Dry Climate, Case of Iran, Tehran, Applied Mechanics and Materials 110-116 (2012) 72-6. doi: https://doi.org/10.4028/www.scientific.net/AMM.110-116.72

[4] Al Horr Y, Arif M, Kaushik A, Mazroei A, Katafygiotou M, Elsarrag E, Occupant productivity and office indoor environment quality: A review of the literature, Building and Environment 105 (2016) 369-89. doi: https://doi.org/10.1016/j.buildenv.2016.06.001

[5] Alrubaih MS, Zain MFM, Alghoul MA, Ibrahim NLN, Shameri MA, Elayeb O, Research and development on aspects of daylighting fundamentals, Renewable and Sustainable Energy Reviews 21 (2013) 494-505. doi: https://doi.org/10.1016/j.rser.2012.12.057

[6] Edwards L, Torcellini P, Literature Review of the Effects of Natural Light on Building Occupants, Office of Scientific and Technical Information (OSTI), 2002, p. 54. Retrieved from: https://www.osti.gov/servlets/purl/15000841, Last Access: 08/11/2019

[7] Beute F, de Kort YAW, Salutogenic Effects of the Environment: Review of Health Protective Effects of Nature and Daylight, Applied Psychology: Health and Well-Being 6 (1) (2014) 67-95. doi: https://doi.org/10.1111/aphw.12019

[8] Aries MBC, Human lighting demands: Healthy lighting in an office environment, Technische Universiteit Eindhoven, Faculteit Bouwkunde, 2005. Retrieved from: https://research.tue.nl/files/1883894/200512454.pdf, Last Access: 08/11/2019

[9] Krüger EL, Tamura C, Trento TW, Identifying relationships between daylight variables and human preferences in a climate chamber, Science of The Total Environment 642 (2018) 1292-302. doi: https://doi.org/10.1016/j.scitotenv.2018.06.164

[10] Boyce P, Hunter C, Howlett O, The benefits of daylight through windows, Rensselaer Polytechnic Institute, Troy., 2003, p. 88. Retrieved from:

http://www.lrc.rpi.edu/programs/daylightdividends/pdf/DaylightBenefits.pdf, Last Access: 28/10/2019

[11] Ne'Eman E, Visual aspects of sunlight in buildings, Lighting Research & Technology 6 (3) (1974) 159-64. doi: https://doi.org/10.1177/096032717400600304

[12] Farley KMJ, Veitch JA, A room with a view: A review of the effects of windows on work and well-being, Institute for Research in Construction, National Research Council Canada, Ottawa, ON, K1A 0R6, Canada, 2001, p. 33. Retrieved from: http://irc.nrc-cnrc.gc.ca/fulltext/rr/rr136/rr136.pdf, Last Access: 27/10/2019

[13] Aries MBC, Veitch JA, Newsham GR, Windows, view, and office characteristics predict physical and psychological discomfort, Journal of Environmental Psychology 30 (4) (2010) 533-41. doi: https://doi.org/10.1016/j.jenvp.2009.12.004

[14] Ko WH, Brager G, Schiavon S, Selkowitz S, Building envelope impact on human performance and well-being: Experimental study on view clarity, UC Berkeley, Center for the Built Environment, 2017. Retrieved from: https://escholarship.org/uc/item/0gj8h384, Last Access: 27/10/2019

[15] Altomonte S, Daylight for energy savings and psycho-physiological well-being in sustainable built environments, Journal of Sustainable Development 1 (3) (2008) 3–16. doi: https://doi.org/10.5539/jsd.v1n3p3

[16] Wang W, Zmeureanu R, Rivard H, Applying multi-objective genetic algorithms in green building design optimization, Building and Environment 40 (11) (2005) 1512-25. doi: https://doi.org/10.1016/j.buildenv.2004.11.017

[17] Diakaki C, Grigoroudis E, Kolokotsa D, Towards a multi-objective optimization approach for improving energy efficiency in buildings, Energy and Buildings 40 (9) (2008) 1747-54. doi: https://doi.org/10.1016/j.enbuild.2008.03.002

[18] Asadi E, da Silva MG, Antunes CH, Dias L, Multi-objective optimization for building retrofit strategies: A model and an application, Energy and Buildings 44 (2012) 81-7. doi: https://doi.org/10.1016/j.enbuild.2011.10.016

[19] Hee WJ, Alghoul MA, Bakhtyar B, Elayeb O, Shameri MA, Alrubaih MS, *et al.*, The role of window glazing on daylighting and energy saving in buildings, Renewable and Sustainable Energy Reviews 42 (2015) 323-43. doi: https://doi.org/10.1016/j.rser.2014.09.020

[20] Manzan M, Padovan R, Multi-criteria energy and daylighting optimization for an office with fixed and moveable shading devices, Advances in Building Energy Research 9 (2) (2015) 238-52. doi: https://doi.org/10.1080/17512549.2015.1014839

[21] Mangkuto RA, Rohmah M, Asri AD, Design optimisation for window size, orientation, and wall reflectance with regard to various daylight metrics and lighting energy demand: A case study of buildings in the tropics, Applied Energy 164 (2016) 211-9. doi: https://doi.org/10.1016/j.apenergy.2015.11.046

[22] Tagliabue LC, Buzzetti M, Arosio B, Energy Saving Through the Sun: Analysis of Visual Comfort and Energy Consumption in Office Space, Energy Procedia 30 (2012) 693-703. doi: https://doi.org/10.1016/j.egypro.2012.11.079

[23] Ochoa CE, Aries MBC, van Loenen EJ, Hensen JLM, Considerations on design optimization criteria for windows providing low energy consumption and high visual comfort, Applied Energy 95 (2012) 238-45. doi: https://doi.org/10.1016/j.apenergy.2012.02.042

[24] Uribe D, Bustamante W, Vera S, Seasonal optimization of a fixed exterior complex fenestration system considering visual comfort and energy performance criteria, Energy Procedia 132 (2017) 490-5. doi: https://doi.org/10.1016/j.egypro.2017.09.676

[25] Carlucci S, Cattarin G, Causone F, Pagliano L, Multi-objective optimization of a nearly zero-energy building based on thermal and visual discomfort minimization using a non-dominated sorting genetic algorithm (NSGA-II), Energy and Buildings 104 (2015) 378-94. doi: https://doi.org/10.1016/j.enbuild.2015.06.064

[26] Iommi M, Daylighting performances and visual comfort in Le Corbusier's architecture. The daylighting analysis of seven unrealized residential buildings, Energy and Buildings 184 (2019) 242-63. doi: https://doi.org/10.1016/j.enbuild.2018.12.014

[27] Carlucci S, Causone F, De Rosa F, Pagliano L, A review of indices for assessing visual comfort with a view to their use in optimization processes to support building integrated design, Renewable and Sustainable Energy Reviews 47 (2015) 1016-33. doi: https://doi.org/10.1016/j.rser.2015.03.062

[28] Halawa E, Ghaffarianhoseini A, Ghaffarianhoseini A, Trombley J, Hassan N, Baig M, *et al.*, A review on energy conscious designs of building façades in hot and humid climates: Lessons for (and from) Kuala Lumpur and Darwin, Renewable and Sustainable Energy Reviews 82 (2018) 2147-61. doi: https://doi.org/10.1016/j.rser.2017.08.061

[29] Omrany H, Ghaffarianhoseini A, Ghaffarianhoseini A, Raahemifar K, Tookey J, Application of passive wall systems for improving the energy efficiency in buildings: A comprehensive review, Renewable and Sustainable Energy Reviews 62 (2016) 1252-69. doi: https://doi.org/10.1016/j.rser.2016.04.010

[30] Yang L, Yan H, Lam JC, Thermal comfort and building energy consumption implications – A review, Applied Energy 115 (2014) 164-73. doi: https://doi.org/10.1016/j.apenergy.2013.10.062

[31] Djongyang N, Tchinda R, Njomo D, Thermal comfort: A review paper, Renewable and Sustainable Energy Reviews 14 (9) (2010) 2626-40. doi: https://doi.org/10.1016/j.rser.2010.07.040

[32] Ghaffarianhoseini A, Berardi U, Ghaffarianhoseini A, Al-Obaidi K, Analyzing the thermal comfort conditions of outdoor spaces in a university campus in Kuala Lumpur, Malaysia, Science of The Total Environment 666 (2019) 1327-45. doi: https://doi.org/10.1016/j.scitotenv.2019.01.284

[33] Ghaffarianhoseini A, Berardi U, Ghaffarianhoseini A, Thermal performance characteristics of unshaded courtyards in hot and humid climates, Building and Environment 87 (2015) 154-68. doi: https://doi.org/10.1016/j.buildenv.2015.02.001

[34] Rupp RF, Vásquez NG, Lamberts R, A review of human thermal comfort in the built environment, Energy and Buildings 105 (2015) 178-205. doi: https://doi.org/10.1016/j.enbuild.2015.07.047

[35] Khatami N, Hashemi A, Improving Thermal Comfort and Indoor Air Quality through Minimal Interventions in Office Buildings, Energy Procedia 111 (2017) 171-80. doi: https://doi.org/10.1016/j.egypro.2017.03.019

[36] Ahmad M, Bontemps A, Sallée H, Quenard D, Experimental investigation and computer simulation of thermal behaviour of wallboards containing a phase change material, Energy and Buildings 38 (4) (2006) 357-66. doi: https://doi.org/10.1016/j.enbuild.2005.07.008

[37] De Rosa M, Bianco V, Scarpa F, Tagliafico LA, Heating and cooling building energy demand evaluation; a simplified model and a modified degree days approach, Applied Energy 128 (2014) 217-29. doi: https://doi.org/10.1016/j.apenergy.2014.04.067

[38] BREEAM. Retrieved from: https://www.breeam.com, Last Access: 08/11/2019

[39] Ghaffarianhoseini A, Rehman AU, Naismith N, Mehdipoor A, Green Building Assessment Schemes: A critical comparison among BREEAM, LEED, and Green Star NZ, International Conference on Sustainable Built Environment (SBE), Seoul, Korea, 2016 of Conference, pp. 474-8. doi: http://bimdirectory.com/Documents/Publications/2016_SELECTED_PROCEEDING_5_GREENBUILDINGa.pdf

[40] Seyedzadeh S, Rahimian FP, Glesk I, Roper M, Machine learning for estimation of building energy consumption and performance: a review, Visualization in Engineering 6 (1) (2018) 5. doi: https://doi.org/10.1186/s40327-018-0064-7

[41] Reinhart CF, Walkenhorst O, Validation of dynamic RADIANCE-based daylight simulations for a test office with external blinds, Energy and Buildings 33 (7) (2001) 683-97. doi: https://doi.org/10.1016/S0378-7788(01)00058-5

[42] Heschong L, Wymelenberg vd, Andersen M, Digert N, Fernandes L, Keller A, *et al.*, Approved Method: IES Spatial Daylight Autonomy (sDA) and Annual Sunlight Exposure (ASE), IES-Illuminating Engineering Society, New York, 2012, p. 14. Retrieved from: https://books.google.com/books?id=KtWbmwEACAAJ, Last Access: 27/10/2019

[43] Dubois M-C, Shading devices and daylight quality: an evaluation based on simple performance indicators, Lighting Research & Technology 35 (1) (2003) 61-74. doi: https://doi.org/10.1191/1477153503li062oa

[44] Krüger EL, Dorigo AL, Daylighting analysis in a public school in Curitiba, Brazil, Renewable Energy 33 (7) (2008) 1695-702. doi: https://doi.org/10.1016/j.renene.2007.09.002

[45] Mardaljevic J, Simulation of annual daylighting profiles for internal illuminance, International Journal of Lighting Research and Technology 32 (3) (2000) 111-8. doi: https://doi.org/10.1177/096032710003200302

[46] Li DHW, Lau CCS, Lam JC, Predicting daylight illuminance by computer simulation techniques, Lighting Research & Technology 36 (2) (2004) 113-28. doi: https://doi.org/10.1191/1365782804li108oa

[47] Hensen JLM, Lamberts R, Building performance simulation for design and operation, Routledge, London, 2012. ISBN: 1134026358

[48] Yu X, Su Y, Chen X, Application of RELUX simulation to investigate energy saving potential from daylighting in a new educational building in UK, Energy and Buildings 74 (2014) 191-202. doi: https://doi.org/10.1016/j.enbuild.2014.01.024

[49] Walsh JWT, The Early Years of Illuminating Engineering in Great Britain, Transactions of the Illuminating Engineering Society 16 (3_IEStrans) (1951) 49-60. doi: https://doi.org/10.1177/147715355101600301

[50] Reinhart CF, Weissman DA, The daylit area – Correlating architectural student assessments with current and emerging daylight availability metrics, Building and Environment 50 (2012) 155-64. doi: https://doi.org/10.1016/j.buildenv.2011.10.024

[51] Paule B, Boutiller J, Pantet S, Sutter Y, Sutter Y, A lighting simulation tool for the new European daylighting standard, Building Simulation and Optimization 2018, Emmanuel College, University of Cambridge, 2018 of Conference. Retrieved from: http://www.ibpsa.org/proceedings/BSO2018/1A-5.pdf, Last Access: 21/10/2019

[52] Yu S-M, Han S-S, Chai C-H, Modeling the Value of View in High-Rise Apartments: A 3D GIS Approach, Environment and Planning B: Planning and Design 34 (1) (2007) 139-53. doi: https://doi.org/10.1068/b32116

[53] Lake IR, Lovett AA, Bateman IJ, Langford IH, Modelling environmental influences on property prices in an urban environment, Computers, Environment and Urban Systems 22 (2) (1998) 121-36. doi: https://doi.org/10.1016/S0198-9715(98)00012-X

[54] Knecht C, Urban nature and well-being: Some empirical support and design implications, Berkeley Planning Journal 17 (1) (2004). doi: https://doi.org/10.5070/BP317111508

[55] Heerwagen JH, Orians GH, Adaptations to Windowlessness: A Study of the Use of Visual Decor in Windowed and Windowless Offices, Environment and Behavior 18 (5) (1986) 623-39. doi: https://doi.org/10.1177/0013916586185003

[56] Aries MBC, Veitch JA, Newsham GR, Physical and psychological discomfort in the office environment, Symposium of the Dutch Light and Health Research Foundation, Eindhoven, The Netherlands, 2007 of Conference, pp. 45-50. Retrieved from: https://research.tue.nl/en/publications/physical-and-psychological-discomfort-in-the-office-environment, Last Access: 20/10/2019

[57] Andersen M, Unweaving the human response in daylighting design, Building and Environment 91 (2015) 101-17. doi: https://doi.org/10.1016/j.buildenv.2015.03.014

[58] LEED v4 for Interior Design and Construction. Retrieved from: https://www.usgbc.org/resources/leed-v4-interior-design-and-construction-current-version, Last Access: 20/10/2019

[59] Daylighting — a guide for designers: Lighting for the Built Environment Chartered Institution of Building Services Engineers, London, United Kingdom, 2014. ISBN: 9781906846480

[60] Standard CED, EN 17037, Daylight of Buildings 2018. Last Access: 28/10/2019

[61] Lee JW, Jung HJ, Park JY, Lee JB, Yoon Y, Optimization of building window system in Asian regions by analyzing solar heat gain and daylighting elements, Renewable Energy 50 (2013) 522-31. doi: https://doi.org/10.1016/j.renene.2012.07.029

[62] Futrell BJ, Ozelkan EC, Brentrup D, Bi-objective optimization of building enclosure design for thermal and lighting performance, Building and Environment 92 (2015) 591-602. doi: https://doi.org/10.1016/j.buildenv.2015.03.039

[63] Vanhoutteghem L, Skarning GCJ, Hviid CA, Svendsen S, Impact of façade window design on energy, daylighting and thermal comfort in nearly zero-energy houses, Energy and Buildings 102 (2015) 149-56. doi: https://doi.org/10.1016/j.enbuild.2015.05.018

[64] Zhang J, Liu N, Wang S, A parametric approach for performance optimization of residential building design in Beijing, Building Simulation (2019). doi: https://doi.org/10.1007/s12273-019-0571-z

[65] Fang Y, Cho S, Design optimization of building geometry and fenestration for daylighting and energy performance, Solar Energy 191 (2019) 7-18. doi: https://doi.org/10.1016/j.solener.2019.08.039

[66] Dino Ipek G, Üçoluk G, Multiobjective Design Optimization of Building Space Layout, Energy, and Daylighting Performance, Journal of Computing in Civil Engineering 31 (5) (2017). doi: https://doi.org/10.1061/(ASCE)CP.1943-5487.0000669

[67] Zhai Y, Wang Y, Huang Y, Meng X, A multi-objective optimization methodology for window design considering energy consumption, thermal environment and visual performance, Renewable Energy 134 (2019) 1190-9. doi: https://doi.org/10.1016/j.renene.2018.09.024

[68] Hiyama K, Wen L, Rapid response surface creation method to optimize window geometry using dynamic daylighting simulation and energy simulation, Energy and Buildings 107 (2015) 417-23. doi: https://doi.org/10.1016/j.enbuild.2015.08.035

[69] Kasinalis C, Loonen RCGM, Cóstola D, Hensen JLM, Framework for assessing the performance potential of seasonally adaptable facades using multi-objective optimization, Energy and Buildings 79 (2014) 106-13. doi: https://doi.org/10.1016/j.enbuild.2014.04.045

[70] Tzempelikos A, Shen H, Comparative control strategies for roller shades with respect to daylighting and energy performance, Building and Environment 67 (2013) 179-92. doi: https://doi.org/10.1016/j.buildenv.2013.05.016

[71] Bader J, Zitzler E, HypE: An Algorithm for Fast Hypervolume-Based Many-Objective Optimization, Evolutionary Computation 19 (1) (2011) 45-76. doi: https://doi.org/10.1162/EVCO_a_00009

[72] Beume N, Fonseca CM, Lopez-Ibanez M, Paquete L, Vahrenhold J, On the Complexity of Computing the Hypervolume Indicator, IEEE Transactions on Evolutionary Computation 13 (5) (2009) 1075-82. doi: https://doi.org/10.1109/TEVC.2009.2015575

[73] Bader J, Deb K, Zitzler E, Faster Hypervolume-Based Search Using Monte Carlo Sampling, in: Ehrgott M, Naujoks B, Stewart TJ, Wallenius J (Eds.), Multiple Criteria Decision Making for Sustainable Energy and Transportation Systems, Springer Berlin Heidelberg, Berlin, Heidelberg, 2010, pp. 313-26. Last Access: 28/10/2019

[74] Octopus. Retrieved from: https://www.food4rhino.com/app/octopus, Last Access: 20/10/2019

[75] Grasshopper. Retrieved from: https://www.grasshopper3d.com/, Last Access: 20/10/2019

[76] Reinhart CF, Jakubiec JA, Ibarra D, Definition of a reference office for standardized evaluations of dynamic façade and lighting technologies, 13th Conference of International Building Performance Simulation Association, Chambéry, France, 2013, pp. 3645-52. Retrieved from: http://www.ibpsa.org/proceedings/BS2013/p_1029.pdf, Last Access: 28/10/2019

[77] ASHRAE, Energy standard for buildings except low-rise residential buildings, Vol. 90, 2007, p. 186. Last Access: 28/10/2019

[78] ASHRAE, ANSI/ASHRAE/USGBC/IES Standard 189.1-2011, Standard for the Design of High-Performance Green Buildings, ASHRAE Atlanta, 2011, p. 114. Retrieved from: https://bcgreencare.ca/system/files/resource-files/PREVIEW_Standard%20for%20the%20Design%20of%20High-Performance%20Green%20Buildings.pdf, Last Access: 27/10/2019

[79] ASHRAE, ANSI/ASHRAE Standard 169-2013, Climatic Data for Building Design, 1791 Tullie Circle, N.E. • Atlanta, GA 30329, 2013. Last Access: 28/10/2019

[80] Weather Data by Location | EnergyPlus. Retrieved from: https://energyplus.net/weather-location/asia_wmo_region_2/IRN//IRN_Tehran-Mehrabad.407540_ITMY, Last Access: 20/10/2019

[81] Rhino 6 for Windows. Retrieved from: https://www.rhino3d.com/, Last Access: 20/10/2019

[82] Dino I, Creative design exploration by parametric generative systems in architecture, Middle East Technical University Journal of the Faculty of Architecture (1) (2012) 207–24. doi: https://doi.org/10.4305/METU.JFA.2012.1.12

[83] Ladybug Tools. Retrieved from: https://www.ladybug.tools/, Last Access: 08/11/2019

[84] EnergyPlus. Retrieved from: https://energyplus.net/, Last Access: 08/11/2019

[85] OpenStudio. Retrieved from: https://www.openstudio.net/, Last Access: 08/11/2019

[86] Konis K, Gamas A, Kensek K, Passive performance and building form: An optimization framework for early-stage design support, Solar Energy 125 (2016) 161-79. doi: https://doi.org/10.1016/j.solener.2015.12.020

[87] Toutou AMY, A Parametric Approach for Achieving Optimum Residential Building Performance in Hot Arid Zone, Faculty of Engineering Department of Architectural Engineering, Alexandria University, 2018. Retrieved from: http://www.secheresse.info/spip.php?article84630, Last Access: 08/11/2019

[88] Marler RT, Arora JS, The weighted sum method for multi-objective optimization: new insights, Structural and Multidisciplinary Optimization 41 (6) (2010) 853-62. doi: https://doi.org/10.1007/s00158-009-0460-7

[89] Python. Retrieved from: https://www.python.org/, Last Access: 20/10/2019

[90] Reinhart CF, Mardaljevic J, Rogers Z, Dynamic Daylight Performance Metrics for Sustainable Building Design, LEUKOS 3 (1) (2006) 7-31. doi: https://doi.org/10.1582/LEUKOS.2006.03.01.001

[91] Ne'Eman E, Hopkinson RG, Critical minimum acceptable window size: a study of window design and provision of a view, Lighting Research & Technology 2 (1) (1970) 17-27. doi: https://doi.org/10.1177/14771535700020010701

[92] Human factors/ergonomics handbook for the design for ease of maintenance, U.S. Department of Energy, Washington, DC; Springfield, VA, 2001. ISBN: 978-1-60119-821-1

[93] Heschong L, Saxena M, Windows and offices: A study of office worker performance and the indoor environment, California Energy Commission, 2003. Retrieved from: http://www.h-m-g.com/downloads/Daylighting/A-9_Windows_Offices_2.6.10.pdf, Last Access: 28/10/2019

[94] Markus TA, The function of windows— A reappraisal, Building Science 2 (2) (1967) 97-121. doi: https://doi.org/10.1016/0007-3628(67)90012-6

[95] Hashemi A, Daylighting and solar shading performances of an innovative automated reflective louvre system, Energy and Buildings 82 (2014) 607-20. doi: https://doi.org/10.1016/j.enbuild.2014.07.086

Appendix A:

Table A.1- Parameters and objective values of random models.

Model in the optimisation process	Parameters						WWR	Objectives				Fitness Function
	WinW	WinH	WinHH	WinSH	WDis	EDis		ASE	sDA	QV	EUI	
	m	m	m	m	m	m	%	%	%	%	kWh/m^2	
5	1.60	0.76	1.71	0.95	1.75	0.15	10.06	8.40	17.65	33.61	91.91	45.21-
61	1.00	1.14	1.90	0.76	1.15	1.75	9.43	9.24	18.49	46.22	91.99	30.56-
102	1.40	1.33	2.28	0.95	1.15	1.35	15.40	13.45	34.45	68.91	90.61	27.50
170	1.60	0.38	1.33	0.95	1.35	0.95	5.03	0.84	10.08	13.45	91.75	63.95-
251	2.00	0.76	1.52	0.76	0.95	0.95	12.57	16.81	21.85	39.50	92.14	53.35-
405	2.60	0.38	1.33	0.95	0.15	1.15	8.17	7.56	17.65	13.45	92.00	68.90-
486	1.20	0.76	1.71	0.95	0.35	1.55	7.54	1.68	13.45	31.09	91.93	38.99-
591	2.60	1.52	2.28	0.76	0.55	0.75	32.69	34.45	47.06	81.51	87.21	38.37
649	1.40	0.38	1.14	0.76	0.55	1.95	4.40	1.68	7.56	11.76	91.75	72.99-
734	2.20	0.76	1.52	0.76	0.95	0.75	13.83	19.33	24.37	39.50	92.20	55.56-
867	3.00	0.57	1.52	0.95	0.55	0.35	14.14	21.85	27.73	27.73	91.87	67.95-
992	1.80	1.14	2.28	1.14	1.75	0.35	16.97	12.61	35.29	56.30	90.33	17.59
1205	1.80	0.95	2.09	1.14	0.75	1.35	14.14	10.92	31.93	49.58	91.21	0.56
1385	1.20	1.33	2.28	0.95	0.35	1.55	13.20	7.56	23.53	52.94	89.32	11.79
1570	2.80	1.14	2.28	1.14	0.95	0.15	26.40	26.05	47.06	58.82	84.33	53.37
1907	1.80	0.95	2.28	1.33	1.75	0.35	14.14	2.52	30.25	47.06	86.41	52.10
2117	2.60	1.14	2.28	1.14	0.55	0.75	24.52	26.89	47.06	58.82	85.27	44.12
2377	2.20	0.76	1.71	0.95	0.75	0.95	13.83	19.33	27.73	39.50	91.92	47.10-
2595	2.40	0.19	0.95	0.76	0.55	0.95	3.77	1.68	7.56	6.72	91.70	78.96-
2879	3.60	0.57	2.28	1.71	0.15	0.15	16.97	1.68	39.50	27.73	87.39	40.16